Physiological responses to light explain competition and facilitation in a tree diversity experiment

Shan Kothari,[1*] Rebecca Montgomery,[2] Jeannine Cavender-Bares[1,3]

[1]Department of Plant and Microbial Biology, University of Minnesota, 140 Gortner Laboratory, 1479 Gortner Ave., St. Paul, MN, 55108
[2]Department of Forest Resources, University of Minnesota, St. Paul, MN, 55108
[3]Department of Ecology, Evolution, and Behavior, University of Minnesota, St. Paul, MN, 55108

*corresponding author
Email: kotha020@umn.edu
Phone: (734) 502-2817

Author contributions: SK conceived the project with JCB, conducted physiological measurements, analyzed and interpreted the data with JCB and RM, and wrote the first draft of the paper. JCB and RM designed the FAB experiment, coordinated annual growth surveys, and contributed to subsequent revisions of the paper.

Abstract

- Ecologists often invoke interspecific facilitation to help explain biodiversity-ecosystem function relationships in plant communities, but seldom test how it occurs. One mechanism through which a species may facilitate others is by ameliorating abiotic stress. Physiological experiments show that a chronic excess of light can cause stress that depresses carbon assimilation. If shading by a plant's neighbors reduces light stress enough, it may facilitate that plant's growth, but if light is often a limiting factor for photosynthesis, shading may have an adverse, competitive effect.
- In a tree diversity experiment, we measured growth rates and photosynthetic physiology of broadleaf tree species across a gradient of light availability imposed by their neighbors. At the extremes, trees experienced nearly full sun (monoculture), or were shaded by nearby fast-growing conifers (shaded biculture).
- Most species had lower growth rates with larger neighbors, implying a net competitive effect. On the other hand, the two most shade-tolerant species (*Tilia americana* and *Acer negundo*) had higher growth rates with larger neighbors, implying a net facilitative effect. Compared to the others, these two species had larger increases in photoinhibition (reduced dark-acclimated F_v/F_m)

across the gradient of increasing light availability, which suggests that they are more vulnerable to chronic light stress. While most species had lower carbon assimilation rates in the shaded biculture treatment, *T. americana* had rates up to 25% higher. *T. americana* also dropped its leaves 3-4 weeks later in shaded bicultures, extending its growing season. We conclude that although large neighbors can cause light limitation in shade-intolerant species, they can also increase growth through abiotic stress amelioration in shade-tolerant species.

- Synthesis: Both positive and negative species interactions in our experiment can be explained by the photosynthetic responses of trees to the light environment created by their neighbors. We show that physiological measurements can help explain the species interactions that underlie biodiversity-ecosystem function relationships. The insights that ecologists gain by searching for physiological mechanisms may help us forecast species interactions under environmental change.

Keywords: Photoprotection; photoinhibition; photosynthetic light-response curves; competition; facilitation; tree diversity; biodiversity and ecosystem function

Introduction

The sun's light powers photosynthesis—the chain of reactions through which plants turn carbon dioxide into the living matter they use to grow and reproduce. A dominant view in plant ecology is that light is often a limiting resource, such that competition for scarce light can govern the fate of plant species (Braun-Blanquet 1932; Canham et al. 1994; Monsi & Saeki 2005; Dybzinski & Tilman 2007). But physiologists have also shown that, when other factors limit photosynthesis, plants commonly absorb more light than they can use. Beyond an initial linear rise with increasing light, photosynthesis begins to saturate, such that additional light contributes little to the plant's carbon gain. By limiting photosynthesis, environmental stresses like water limitation, cold temperatures, or nutrient-poor conditions can exacerbate the excess of light (Fig. 1; Long et al. 1994; Demmig-Adams & Adams 1992).

Light is thus both an essential resource and a potential stressor. A chronic excess of light can cause plant cells lasting oxidative damage, especially to Photosystem II (PSII). Oxidative damage reduces the efficiency of photosynthesis and can be costly to repair, but plants can avoid it using mechanisms of photoprotection (Murchie & Niyogi 2011). These mechanisms include biochemical pathways that safely dissipate excess light as heat—most notably, the xanthophyll cycle. They also include structural means to avoid absorbing too much light, such as self-shading canopies, reflective leaves, or steep leaf angles (Lovelock et al. 1992; Pearcy et al. 2005; Kothari et al. 2018).

Each form of photoprotection comes with costs. Once induced, many forms of biochemical photoprotection are slow to reverse. Even when light stress subsides, these mechanisms may continue to suppress photosynthesis for some time, making them costly under fluctuating light (Demmig-Adams & Adams 2006; Kromdijk et al. 2016). Structural mechanisms like self-shading may be costly under low ambient light. In general, photoprotective mechanisms are stronger under environmental conditions that put plants at risk of damage, including high light (Montgomery et al. 2008) and cold or dry climate (Cavender-Bares 2007; Savage et al. 2009; Wujeska et al. 2013; Ramírez-Valiente et al. 2013). Under such conditions, plants need strong photoprotection to prevent even more costly damage.

Depending on how well-protected a plant is, prolonged exposure to excess light can still cause enough damage to reduce carbon assimilation rates (Egerton et al. 2000; Howell et al. 2002; Murchie & Niyogi 2011). Consistent with Long et al. (1994), we use the term "photoinhibition" to describe a drop in carbon assimilation caused by either photodamage or slow-reversing biochemical photoprotection. Bright sunlight causes photoinhibition directly by exposing leaves to more radiation—but it also acts indirectly by altering other microclimatic conditions like temperature, soil moisture, and vapor pressure deficit (VPD; Björkman & Powles 1984). For example, high VPD can cause stomata to close, which limits the use of light for photosynthesis; without an energetic sink, the resulting excess of light can then cause photoinhibition, which limits photosynthetic capacity even further. Belowground competition may also make plants more vulnerable to photoinhibition by depleting resources they need for photosynthesis. Because these stresses vary along environmental gradients, photoinhibition and photoprotective investments are likely to affect the distribution and persistence of plant populations (Külheim et al. 2002).

Given that excess light can cause stress, it may be that one plant species can facilitate another through shading. Whether a plant receives net costs or benefits from its neighbors' shade depends on the balance of two effects:

1. Reduction in light available at any instant, which can increase the frequency and severity of photosynthetic light limitation; and,
2. Avoidance of chronic light stress, which can increase photosynthesis at any given light level.

Monteith et al. (1977) defined light-use efficiency (LUE) as net photosynthesis divided by the amount of photosynthetically active radiation (PAR) absorbed. Chronic photoinhibitory stress lowers LUE, such that plants do less with the amount of light they absorb. Shade helps when, across time, the gain of avoiding chronic stress is greater than the loss caused by potential light limitation. Changes in light availability alter the horizontal position along a photosynthetic light-response curve at each moment; changes in LUE alter the shape of the curve such that plants assimilate more or less carbon at a given position along the curve (Fig. 1). Both effects must be considered together to test whether shading helps or hurts.

The species interactions that result from shading could help to explain the results of experiments that manipulate biodiversity, including tree diversity. Experimental and observational research alike has shown that biodiversity often promotes ecosystem functions such as productivity (Tilman et al. 2014). In forests, this trend has been shown in both experimental (Potvin & Gotelli 2008; Tobner et al. 2016; Grossman et al. 2017; Williams et al. 2017; Huang et al. 2018; Zemp et al. 2019) and observational (Gamfeldt et al. 2013; Liang et al. 2016; Oehri et al. 2017) data, across temperate (Tobner et al. 2016; Grossman et al. 2017; Williams et al. 2017), subtropical (Huang et al. 2018), and tropical (Potvin & Gotelli 2008; Zemp et al. 2019) biomes. These positive relationships are robust to variation in climate, successional stage, and other factors (reviewed in Grossman et al. 2018; Ammer 2018).

One of the possible drivers of positive biodiversity-productivity relationships is interspecific facilitation (Wright et al. 2017; Barry et al. 2018). In biodiversity experiments, patterns of productivity within species or functional groups can sometimes serve as evidence that some species facilitate others (Mulder et al. 2001; Fichtner et al. 2017), but they cannot tell us the physiological mechanisms that allow facilitation to occur. Ecologists may need to understand these mechanisms to forecast species interactions and productivity under environmental change (Wright et al. 2017; Barry et al. 2018).

Here, we tested whether the shade created by tree crowns can facilitate the carbon assimilation and growth of neighboring trees in the Forests and Biodiversity (FAB) experiment at Cedar Creek Ecosystem Science Reserve (East Bethel, MN). We asked: Do some species aid others by shielding them from stress caused by intense sunlight? In particular, we sought to test whether slow-growing, shade-tolerant broadleaf trees might be facilitated by adjacent fast-growing conifers (Table 1). We addressed this question by measuring the physiology and woody growth of broadleaf species across plots that vary in species composition. If certain species do benefit from the shade of their neighbors, we would expect individuals with larger neighbors to have higher growth and carbon assimilation rates. We also posed the hypothesis that trees exposed to high light would use structural and biochemical photoprotective mechanisms more than trees shaded by their neighbors. If true, this finding would imply that trees

growing in high light must invest in photoprotection to avoid damage, reinforcing the claim that light stress influences the interactions within these communities.

Methods

Experimental design

The Forests and Biodiversity (FAB) experiment began in 2013 and comprises 142 4 × 4 m plots, each planted with 64 trees in a 0.5 × 0.5 m grid. The experiment has three blocks, each with 49 plots arranged in a 7 × 7 square. Neighboring plots within a block share a boundary. Each plot is planted with 1, 2, 5, or 12 species from a pool of 12 total species, including four evergreen conifers with needle-like leaves and eight deciduous angiosperms with broad leaves (Table 1). Except for five-species plots, each distinct species composition has a replicate in each block. All species in a plot have nearly equal frequency, and the placement of species within a plot is random. The experimental design is described in greater detail in Grossman et al. (2017).

The mean relative growth rate in monoculture during the first three years varied dramatically among species, being highest in conifers and *B. papyrifera* (Table 1). During these first three years, Grossman et al. (2017) found that diverse plots overyield in productivity—their growth is greater than a weighted average of the constituent species' growth in monoculture. Using the partition of Loreau & Hector (2001), most of this overyielding came from complementarity effects—which are often interpreted as a result of synergistic interactions among species—rather than selection effects.

Tree growth

We surveyed tree growth in late fall of each year. For all living trees, we measured diameter and height to the tallest leader. We measured basal diameter (5 cm from the ground) for trees less than 137 cm tall, and diameter at breast height for trees more than 137 cm tall. For a subset of individuals, we measured both diameters. To predict basal diameter when it was not measured, we used linear

relationships predicting basal diameter from the height of the same individual in the same year and the basal diameter in the previous year.

We estimated woody stem volume as $V = \pi r^2 h$, where h is height and r is the basal radius (half the basal diameter). This assumes each tree stem is a cylinder, an assumption that has been used and justified in other tree diversity studies in the absence of system-specific allometric equations (Tobner et al. 2016; Williams et al. 2017). We then calculated the yearly relative growth rate (RGR) between 2016 and 2018 as $RGR = (\ln V_{2018} - \ln V_{2016})/2$ (Hoffman & Poorter 2002). We chose 2016 as a starting point because no replanting of dead trees occurred after that point.

For each tree, we also calculated the average stem volume of its eight neighbors (in cardinal and intercardinal directions) in 2018 as a proxy for the intensity of aboveground interactions. We tested how focal individual growth changes with neighbor size using ordinary least-squares (OLS) regression. We also tested whether any species showed hump-shaped responses to neighbor size using the two-lines test (Simonsohn 2018). Neighbors were sometimes missing, either because of mortality or because the focal individual was on the edge of the experiment. In these cases, we assigned that neighbor a volume of zero.

Photosynthetic physiology

We measured dark- and light-acclimated chlorophyll fluorescence parameters and reflectance spectra in all eight broadleaf species. We also measured photosynthetic light-response curves among four focal species (*A. rubrum*, *B. papyrifera*, *Q. ellipsoidalis*, and *T. americana*).

For physiological measurements, we focused on plots belonging to one of three treatments: (1) monocultures of broadleaf species ("monoculture"); (2) bicultures comprising one broadleaf and one conifer species ("shaded biculture"); and (3) twelve-species plots ("twelve-species") (see Fig. S1 for sample images). For each species in each treatment, we measured physiological parameters on six individuals—two in each of three plots. Neither *A. negundo* nor *Q. macrocarpa* was planted with a conifer in any biculture. We used *B. papyrifera* as a shaded biculture partner for *Q. macrocarpa* because it is a fast-growing species that creates shade. We omitted the shaded biculture treatment for *A. negundo*.

When possible, we chose the same trees within a plot for each kind of physiological measurement so that we could compare these aspects of physiology within individuals.

Photosynthetic light-response curves

We measured photosynthetic light-response curves from the four focal species during July 2018 using an LI-6400 gas exchange system (LI-COR BioSciences, Lincoln, NE) with a 6400-40 Leaf Chamber Fluorometer head. From each tree (n = 72 total), we selected a fully expanded upper leaf with no visible sign of disease or herbivory. We noted the angle of each leaf relative to horizontal (to the nearest 15˚) before beginning measurements. Each curve had nine steps in descending order of brightness: 2000, 1500, 1000, 500, 200, 100, 50, 20, and 0 µmol m^{-2} s^{-1}. We also measured relative electron transport rate (ETR) using chlorophyll fluorescence at each light level. We maintained favorable conditions inside the chamber during each measurement. Following each curve, we removed the leaf to measure leaf mass per area (LMA) using a balance and a flatbed scanner. Further details about light-response curve procedures and ETR calculations can be found in the Supplemental Methods. Finally, we estimated parameters like the light-saturated photosynthetic rate (A_{sat}) by fitting a non-rectangular hyperbolic model (Lobo et al. 2013) to each light-response curve using *R* code written by Nick Tomeo, available at: https://github.com/Tomeopaste/AQ_curves.

We aimed to determine how carbon assimilation rates vary with the ambient light level, which we define as the photosynthetic photon flux density (PPFD) in an open field adjacent to the experiment. For most leaves we measured, *in situ* light availability is lower than the ambient light level, mainly because each tree is shaded by its neighbors. Following Howell et al. (2002), we transformed each measured light-response curve along the *x*-axis based on how much light it receives as a proportion of ambient light. This procedure lets us estimate carbon assimilation as a function of ambient light.

For example, if the topmost leaves of a tree only receive 50% of ambient light, we would stretch its light-response curve two-fold along the *x*-axis. For this tree, the realized assimilation rate we estimate at an ambient (or open field) PPFD of 2000 µmol photons m^{-2} s^{-1} would be the assimilation rate at a leaf-

level PPFD of 1000 μmol m^{-2} s^{-1}. We estimated the scaling factor for each individual as $RLA \times \cos(\theta)$, where *RLA* is relative light availability (see *Light availability*) and θ is the leaf angle from horizontal. (Taking the cosine of θ approximately corrects for the reduction in horizontally projected leaf area in steeply inclined leaves when the sun is directly overhead, as simplified from Ehleringer & Werk [1986].) We used this procedure on each fitted curve in order to compare across treatments in a way that accounts for the variable light intensity each individual receives. We refer to the unscaled photosynthetic light-response curves as a function of the leaf chamber PPFD as *chamber light-response curves*, and the rescaled light-response curves as a function of ambient PPFD as *ambient light-response curves*.

Finally, we used ambient light-response curves to estimate carbon assimilation by top leaves throughout July. We used an hourly averaged time series of ambient solar radiation from Carlos Avery Wildlife Management Area in Columbus, MN, 13.6 km away from the study site. Following Udo and Aro (1999), we assumed that each Watt m^{-2} of solar radiation has about 2.08 μmol photons m^{-2} s^{-1} of PAR. By using these data as inputs to the ambient light-response curves, we estimated carbon assimilation integrated over the month of July, as Posada et al. (2009) do at daily scales. This procedure assumes that the photosynthetic response to light remains constant, and is not affected by factors like leaf temperature and stomatal closure. While this assumption is never quite true, we consider it a useful way of estimating the consequences of realistic fluctuations in light. We compared treatments within species using ANOVA.

Throughout the paper, we express assimilation per unit of leaf dry mass because we aim to determine the plants' return on investment in biomass. As expected, leaves growing in low light environments tended to have lower LMA in most species (Fig. S2; Poorter et al. 2019), and expressing data on a mass basis accounts for these large differences in construction cost. We also express stomatal conductance (g_s) and electron transport rate (ETR) on a mass basis to compare them with assimilation rates, with the caveat that both processes typically occur near the leaf surface.

Instantaneous chlorophyll fluorescence, pigments, and spectral reflectance

In all eight broadleaf species, we measured chlorophyll fluorescence parameters using an FMS2 pulse-modulated fluorometer (Hansatech Instruments Ltd., Norfolk, UK) over two days in late July (*n* = 138 total). We measured dark- and light-acclimated parameters at the same spot on the same leaves. We attached opaque clips to leaves in the evening before measuring dark-acclimated F_v/F_m within two hours after sunrise. This parameter describes the maximum quantum yield of PSII and is a general index of photoinhibition, including sustained photoprotection (Murchie & Lawson 2013). We then took light-acclimated measurements between 12:00 and 14:00 each day. The protocol involved the following steps: actinic light at 1000 µmol m^{-2} s^{-1} for 15 seconds, a saturating pulse, and two seconds of far-red light. We exposed all leaves to the same actinic light because we aimed to assess photoprotective capacity under comparable light conditions, even though each tree had a different light environment.

From these data, we estimated qN, a parameter that indicates how much a plant relies on photoprotective dissipation (non-photochemical quenching) under the imposed actinic light. This parameter is correlated with de-epoxidation of xanthophyll cycle pigments (Watling et al. 1997; Cavender-Bares and Bazzaz 2004). Following Kramer et al. (2004), we also calculated the quantum yields Φ_{PSII}, Φ_{NPQ}, and Φ_{NO}, which sum to 1. These three parameters are the proportions of light energy dissipated by photosynthetic chemistry, non-photochemical quenching, and non-regulated dissipation. The last is a crucial parameter because it represents light that a plant cannot dissipate safely; this portion of the absorbed light may contribute to photodamage. The Supplemental Methods contain formulas for all parameters and justifications for our choices in data analysis.

On separate top leaves of the same trees, we measured reflectance spectra (350-2500 nm) using a PSR+ 3500 field spectroradiometer (Spectral Evolution, Lawrence, MA). We used these spectra to calculate the photochemical reflectance index (PRI), a two-band index that most strongly indicates carotenoid : chlorophyll ratios (Gamon et al. 1992; Wong & Gamon 2015; Gitelson et al. 2017). This index is calculated as PRI = $(R_{531} - R_{570}) / (R_{531} + R_{570})$, where R_n is reflectance at a wavelength of *n* nm. Low PRI tends to indicate high carotenoid : chlorophyll ratios. We used OLS regression to estimate

species-specific responses of PRI and each chlorophyll fluorescence parameter against relative light availability (see *Light availability*).

To understand how photoprotective allocation varies with adaptations to shade, we used shade tolerance values that Niinemets & Valladares (2006) compiled on a five-point scale based on prior literature. Higher values along this scale indicate that plants are able to grow in lower light conditions.

Phenology

We monitored the timing of leaf abscission in monoculture and shaded biculture plots for *T. americana* to assess whether shade could delay senescence and abscission, extending the period for carbon gain (Cavender-Bares et al. 2000). In early August, we surveyed 120 *T. americana* trees (60 in monoculture, 60 in shaded biculture) to determine the proportion of leaves that had fallen based on how many of the top five axillary buds lacked a leaf. From each of these trees, we marked a single leaf and returned every 1-2 weeks to monitor its senescence. We assessed each leaf on a binary basis (senesced or not) based on whether it had at least 50% remaining green leaf area. We chose this criterion as a simple proxy for the continuous scale used by Cavender-Bares et al. (2000). Based on the initial survey and the repeated surveys of marked leaves, we tracked the proportion of leaves that had senesced over time. To ensure that leaves were photosynthetically active until near the point of senescence, we collected a one-time measurement of dark-acclimated F_v/F_m in mid-September among remaining leaves.

We also performed a one-time measurement of 60 (30 per treatment) *A. rubrum* plants on October 1, using the same protocol we used to do our initial early August survey of *T. americana*. We aimed for this survey to help test whether our results hold across species.

Water potential

Water deficits—even moderate ones—can reduce carbon gain by causing stomata to close (Brodribb et al. 2003). To assess how our treatments affected water status, we measured leaf water potential using a Scholander pressure bomb. We measured pre-dawn water potential (Ψ_{PD}) in all eight

broadleaf species (n = 96) and midday water potential (Ψ_{MD}; between 12:00 and 14:00) in only the four focal species (n = 48). In these measurements, we included monoculture and shaded biculture treatments, except in *A. negundo*, where we used the twelve-species treatment in place of the absent shaded biculture treatment. We removed leaves and immediately placed them in impermeable plastic bags with wet paper towels. We carried leaves in coolers to be measured indoors within 90 minutes.

Because we only intended to test whether there was a general tendency across species for water potential to vary with light, we included species as a random effect and light availability as a fixed effect in regression models for both Ψ_{PD} and Ψ_{MD}. We calculated p-values using Satterthwaite's degrees of freedom method in the *lmerTest* package (Kuznetsova et al. 2017), noting that such values should be interpreted conservatively.

Leaf angles

Leaf angle is a key control on light exposure because more vertical leaves intercept less light when the sun is directly overhead, and allow light to percolate deeper into the canopy. As a result, steep leaf angles can be a key structural strategy for avoiding light, temperature, and water stress (Valladares & Pugnaire 1999; Werner et al. 1999; Pastenes et al. 2004; Valiente-Banuet et al. 2010). We predicted that trees in monoculture would have steeper leaf angles than those in other treatments because they need to avoid excess light. From each of three species (*A. rubrum*, *Q. ellipsoidalis*, and *T. americana*), we randomly selected five individuals from each of six plots—three from monoculture treatments, three from shaded bicultures (n = 15 per species × treatment). On these individuals, we measured the leaf angle from horizontal of the top five leaves in the crown to the nearest 15˚.

Because angles of leaves within individuals may be non-independent, we tested whether treatments differ using a mixed-effects model with treatment as a fixed effect and individual tree nested within plot as a random effect. Deviations from horizontal in either direction can reduce light interception, so we used the absolute value of leaf angle as the dependent variable in statistical analyses. We again calculated p-values using Satterthwaite's degrees of freedom method.

Environmental data

Light availability

On a cloudy day with diffuse light conditions, we measured light interception above each tree selected for this study (n = 138) using an AccuPAR LP-80 ceptometer (METER Group, Pullman, WA). We took the mean of two to four PAR measurements in the open and the mean of two measurements directly above the topmost leaf of each tree. By calculating a ratio of these values, we could calculate the percent of light transmitted to the top of each tree. We called this value *relative light availability* (RLA). This value is typically well-correlated with the percentage of ambient light available over much longer time-scales (Parent & Messier 1996).

Soil water content

We collected a one-time measurement of soil volumetric water content in mid-August using a FieldScout Time-Domain Reflectometer 350 (Spectrum Technologies, Inc., Aurora, IL). This single measurement followed six days from the last rain. At midday, we collected and averaged three measurements in each of 32 plots, spanning monocultures of the four core broadleaf species, shaded bicultures, and twelve-species plots.

Air temperature

For nine days during early September, we set out four Thermochron iButtons (model DS1921G; Maxim Integrated Products, Sunnyvale, CA, USA) in shaded plots and two in twelve-species plots, setting them to log air temperature hourly. Each iButton was suspended on mesh inside a 1 m-tall PVC pipe that was capped with an elbow to shield against solar irradiance. We compared these data to air temperature measured hourly under open, sunny conditions at the Cedar Creek LTER weather station about 0.77 km away. We assumed that data from this station would be representative of air temperature in non-shaded areas. We ignored nighttime and early morning (20:00-08:00 h) readings because iButtons may have been influenced by evaporative cooling of condensed water droplets.

Results

Tree size and growth

Neighborhood-scale relationships between focal individual RGR and total neighbor stem volume were noisy but often highly significant (Fig. 2). In most species, individuals with larger neighbors had lower RGR, including in *A. rubrum* (R^2 = 0.033, p <10^{-5}), *Q. alba* (R^2 = 0.038, p <10^{-6}), *Q. ellipsoidalis* (R^2 = 0.030, p <10^{-5}), *Q. macrocarpa* (R^2 = 0.027, p <10^{-5}), and *Q. rubra* (R^2 = 0.056, p <10^{-9}). On the other hand, some species grew faster with larger neighbors, including *A. negundo* (R^2 = 0.018, p < 0.005) and *T. americana* (R^2 = 0.019, p <10^{-4}). *B. papyrifera* showed no significant relationship with neighbor size. No species had a hump-shaped response. These results are qualitatively unchanged by eliminating trees on the edge of the experiment or incorporating plot as a random effect.

Although these individual-level effects are noisy, they show strong tendencies in average stem growth across the full range of neighbor size. Imagine two *T. americana* trees that begin at the same size in 2016: One in monoculture, where the average neighbor in 2018 is 573 cm^3, and one growing in a shaded biculture with *Pinus strobus*, where the average neighbor is 2175 cm^3. The individual-level regression predicts that after two years, the average *T. americana* in the shaded biculture would be 39.7% larger because of the difference in mean RGR. Or, consider *Q. rubra*, which had the strongest negative response to neighbor size: We predict that an average tree in the shaded biculture would be 39.1% smaller than in monoculture. Because these figures assume that treatments have not developed any average size differences by 2016, they may underrepresent the true differences in size that have accumulated, and may continue to accumulate with time.

We can also aggregate these observations to the plot scale—for example, by considering the RGR of summed stem volume of each species in each plot (Fig. 2). (This approach is distinct from an average of individual RGRs, which assigns equal weight to small and large individuals.) Although aggregation leaves less power to detect significant relationships, the relationships we find here explain much more of the variation in growth across plots, including negative RGR responses to average neighbor size in *Q.*

alba (R^2 = 0.311, $p < 0.001$) and *Q. macrocarpa* (R^2 = 0.174, $p < 0.01$) and a positive response in *T. americana* (R^2 = 0.282, $p < 0.001$).

Trees that died between 2016 and 2018 dropped out of our individual-level analyses of RGR because their stem volume was 0 in 2018, making it impossible to calculate RGR. To see whether mortality could alter our conclusions, we also performed statistical analyses on untransformed growth in stem volume from 2017 to 2018, in which we alternately (1) treated mortality as a decline in volume to 0, or (2) removed trees that died from analyses. The rate of mortality was low between 2016 and 2018 (~7.5%), and accounting for mortality makes no qualitative difference when considering absolute growth as the response variable (Fig. S3).

Photosynthetic physiology

Photosynthetic light-response curves

In three out of the four focal species (*Q. ellipsoidalis*, *A. rubrum*, and *T. americana*), photosynthetic rates (per unit dry mass) were higher in shaded biculture and twelve-species treatments than in monoculture at any given chamber light level (Fig. 3, left). In the lone pioneer species, *B. papyrifera*, photosynthetic rates in shaded biculture were lower than in the other two treatments.

The rate of photosynthesis is often limited either by ETR or by the RuBP carboxylation rate, which in turn is often limited by stomatal diffusion of CO_2 (Farquhar et al. 1980). In our data, both ETR and stomatal conductance (g_s) increase with light availability (Fig. S4). (ETR tends to decline at very high light levels, especially in shaded treatments, perhaps because of acute photoinhibition.) Within each species, the rank-order of treatments in photosynthetic rates, ETR, and g_s are broadly congruent. One exception is that *T. americana* in shaded biculture has much higher g_s than in twelve-species or monoculture plots, despite having slightly lower photosynthetic rates than in twelve-species plots.

Compared to chamber light-response curves, the picture that emerges from ambient light-response curves is more complex (Fig. 3, right). In *B. papyrifera*, the assimilation rate was still lowest across light levels in the shaded biculture treatment. In late-successional *T. americana*, the assimilation

rate was higher in shaded biculture and twelve-species treatments by up to 25% compared to monoculture across most light levels. In the other two species, the assimilation rate was highest in monoculture at low light, but twelve-species and (in *Q. ellipsoidalis*) shaded biculture plots intersected and surpassed monocultures when enough light was available. *A. rubrum* and *Q. ellipsoidalis* grew less and had lower relative light availability (RLA) in shaded bicultures than *T. americana* (Fig. S2), so their assimilation rates dropped considerably more in ambient light-response curves.

Using a time series of solar radiation, we estimated total assimilation rates in July 2018 based on each ambient light-response curve (Fig. S5). We found that trees would have lower total assimilation in shaded biculture than in monoculture in *A. rubrum* (ANOVA; $p = 0.008$) and *B. papyrifera* ($p = 0.002$). In both species, trees in twelve-species plots did not differ from those in monoculture. In the other two focal species, there were no significant differences at all among treatments. In these integrated estimates, the cost of shade seem larger than one might suppose from looking only at instantaneous assimilation rates under high ambient light. We attribute these high costs to low light levels: PPFD was under 500 μmol m^{-2} s^{-1} more than 60% of the time. It is under such dim conditions that trees in monoculture most outperform those in shaded biculture.

Instantaneous chlorophyll fluorescence, pigments, and spectral reflectance

Among all eight species but early-successional *B. papyrifera*, dark-acclimated F_v/F_m declined as RLA increased (Fig. 4), confirming that high light exposure causes photoinhibition. Among the four focal species, dark-acclimated F_v/F_m is positively correlated with A_{sat}, the light-saturated photosynthetic rate (OLS regression; $R^2 = 0.44$; $p < 10^{-9}$; Fig. 5); slopes are not significantly different among species. The correlation suggests that photoinhibitory declines in PSII efficiency may explain why three out of four species had higher A_{sat} in shaded bicultures and twelve-species plots.

In most species, qN rose with RLA, which shows that trees that grow in high light use non-photochemical quenching more to dissipate excess light (Fig. 4). Two species were clear exceptions: In *T.*

americana and *A. negundo*, qN was nearly invariant across the range of light availability, showing that these species do not increase photoprotective dissipation with light.

Extracting the species-specific slopes of dark-acclimated F_v/F_m against RLA, we find that that the species with the greatest decline in F_v/F_m are the most shade-tolerant (Fig. 5; $R^2 = 0.601$; $p = 0.025$). Similarly, more shade-tolerant species have less (or no) increase in qN with light availability ($R^2 = 0.619$; $p = 0.022$). The trends suggest that shade-tolerant species may have large increases in photoinhibition across the light gradient because they fail to upregulate their non-photochemical quenching.

To illustrate why shade-tolerant species show such large increases in photoinhibition with light, consider Φ_{PSII}, Φ_{NPQ}, and Φ_{NO}—the quantum yields of PSII photochemistry, non-photochemical quenching, and non-regulated dissipation (Fig. S6). We set aside *B. papyrifera*, which grows fast enough that it is seldom truly shaded. In most other species, Φ_{NO} decreases with light in the growth environment (Fig. 4). Plants growing in the full sun can either use light at 1000 μmol photons m^{-2} s^{-1} for photochemistry, or dissipate much of the remainder through non-photochemical quenching, keeping Φ_{NO} close to the oft-cited theoretical minimum of ~0.17 (Tietz et al. 2017). But in *T. americana* and *A. negundo*, Φ_{NO} is nearly equal across the gradient of light availability, which may explain why these species show such large declines in dark-acclimated F_v/F_m with light. Sun-exposed trees of all species are more photoinhibited because they experience high light levels more often, but the risk is especially great for the shade-tolerant species.

PRI declined with increasing light availability in all species, which supports the idea that trees in monoculture allocate more to carotenoids (Fig. 4). Although this relationship had remarkably consistent slopes and intercepts across nearly all species, *B. papyrifera* had higher PRI at all light levels within its narrow domain.

Phenology

In *T. americana*, leaf abscission in monoculture began in early August, and more than half of all leaves had senesced by September 3 (Fig. 6). In shaded bicultures, more than 90% of leaves remained by

September 3, and no survey found greater than 50% senescence until October 1. We assigned the senescence date of each leaf as the date of the first survey by which it had senesced; using this response variable, leaves in monoculture senesced much earlier than those in shaded cultures (t-test; $p < 10^{-11}$). These results suggest that leaves in shaded bicultures had, on average, one additional month for carbon gain. Here, we assume that leaves in shaded biculture did not downregulate photosynthesis any longer before abscission than those in monoculture. This assumption was supported by mid-September measurements of dark-acclimated F_v/F_m. In shaded biculture, dark-acclimated F_v/F_m averaged 0.745 at this point, which was higher than the mean among remaining monoculture leaves, 0.642 (t-test; $p = 0.061$).

Our one-time measurement of *A. rubrum* leaves in early October confirmed that this pattern is not limited to *T. americana*. *A. rubrum* trees in shaded biculture plots retained about 56% of their leaves, while those in monoculture retained only 10% (t-test; $p < 10^{-4}$).

Water potential

We removed two data points, one in each treatment, with Ψ_{PD} more negative than -0.8 MPa on the grounds that they may have been subject to measurement error. Across treatments, the mean Ψ_{PD} and Ψ_{MD} were -0.15 and -1.29 MPa. Ψ_{PD} increased with light availability ($p < 10^{-5}$), making it less negative in monocultures than shaded bicultures by an average of 0.07 MPa. This result holds even including the outliers ($p = 0.013$). By midday, the pattern reversed; Ψ_{MD} declined with light availability ($p < 10^{-4}$), making it more negative in monocultures than shaded bicultures by an average of 0.33 MPa.

Leaf angles

Among each of the three species whose leaf angles we measured, leaves were more horizontal in the shaded biculture treatment (Fig. 7). The size of this fixed effect varied among species: 9.0˚ in *Q. ellipsoidalis* ($p = 0.037$), 22.0˚ in *A. rubrum* ($p = 0.022$), and 25.0˚ in *T. americana* ($p = 0.002$). Because *T. americana* leaves usually drooped downward in monoculture, leaf angles became less negative in the shade. In *Q. ellipsoidalis*, whose leaves were often inclined upward in monoculture, leaf angles became

less positive in the shade. In *A. rubrum*, leaf angles were inclined both up and down in monoculture, but varied less in either direction in the shade.

Environmental factors

In our survey, soil moisture varied among treatments (ANOVA; $p < 0.01$); it was lowest (5.7%) in shaded biculture plots and highest (7.2%) in broadleaf monoculture plots. We found that daytime air temperature in the open was higher than in shaded bicultures or twelve-species plots at 62.5% of hourly log-points during the nine-day logging period. The air temperature in monocultures averaged 1.03˚ C higher over this period.

Discussion

We investigated how species interactions in a tree diversity experiment might emerge from the physiological responses of trees to the light environment created by their neighbors. We found that two species (*A. negundo*, *T. americana*) grew faster on average with larger neighbors, while five (*A. rubrum*, *Q. alba*, *Q. ellipsoidalis*, *Q. macrocarpa*, and *Q. rubra*) grew slower. The two species with positive responses to neighbor size were shade-tolerant and faced a high risk of photoinhibition in high light, which could reduce carbon assimilation in monoculture. The five species with negative responses were shade-intolerant, increased their non-photochemical quenching in high light, and tended to have lower carbon assimilation in shaded bicultures. The divergent responses of these two groups of species appear to be driven in part by their tolerance to excess light. Here, we interpret these patterns further.

Interpreting patterns of stem growth

The stem growth data show that larger neighbors increase aboveground growth in *T. americana* and *A. negundo*, the most shade-tolerant species. We interpret this pattern as a result of facilitation, perhaps through abiotic stress amelioration. Because we did not measure root growth, we cannot rule out the chance that this trend is caused by a shade avoidance response that increases allocation to shoots

compared to roots in the shade (Schall et al. 2012). Nevertheless, the idea that much of this effect is facilitative is supported both by physiological data and by other studies wherein shade increased combined root and shoot biomass (e.g. Ryser & Eek 2000; Semchenko et al. 2012).

In contrast, focal individuals of all four *Quercus* species and *A. rubrum* grew less when surrounded by larger neighbors. In these species, neighborhood interactions are dominated by competition, potentially both aboveground and belowground. The fact that soil moisture was lowest in our dense-growing shaded biculture plots suggests the occurrence of belowground competition. The pioneer species *B. papyrifera*, whose leaves had lower photosynthetic rates in the shaded biculture, had a neutral response to neighbor size, perhaps because its rapid growth allowed it to overtop its neighbors. Aside from *B. papyrifera*, we found, as in prior research (Montgomery et al. 2010), that more shade-tolerant species show more facilitative responses to being shaded.

Physiology of carbon gain

We chose our four focal species along a gradient from early-successional, shade-intolerant *B. papyrifera*, to mid-successional *A. rubrum* and *Q. ellipsoidalis*, to late-successional, shade-tolerant *T. americana* (Braun 1950). This successional gradient aligns with the varied consequences of shade for carbon gain across species. Growing in a shaded biculture can either: (1) decrease assimilation rates (compared to monoculture) at all ambient light levels, as in *B. papyrifera*; (2) decrease assimilation under low ambient light, but increase it under high light, as in *A. rubrum* and *Q. ellipsoidalis*; or (3) increase assimilation rates at most ambient light levels, as in *T. americana*. Our finding that carbon gain in *T. americana* can increase under shade is reinforced by Carter and Cavaleri (2018), who find that its photosynthetic rates may increase down vertical gradients from the upper canopy to the sub-canopy.

The untransformed light-response curves can help us identify the causes of these patterns. As a function of leaf chamber PPFD—without penalizing for lowered light availability—three of our four species (*A. rubrum*, *Q. ellipsoidalis*, and *T. americana*) had higher photosynthetic rates in the shaded biculture and twelve-species treatments than in monoculture (Fig. 3, left). In all species except early-

successional *B. papyrifera*, dark-acclimated F_v/F_m declines with light availability. This trend suggests a role for photoinhibition in determining photosynthetic rates because dark-acclimated F_v/F_m correlates with A_{sat}. Because photoinhibition most often occurs through damage or downregulation of PSII, it is usually thought to depress photosynthesis by lowering ETR. But both ETR and stomatal conductance mirror the patterns in photosynthesis across treatments in chamber light-response curves (Fig. S4), so both may have some role in explaining why most species had lower photosynthesis in monoculture.

Given that light availability fluctuates—diurnally, seasonally, and with cloud cover—the treatment that performs best may also vary from moment to moment. We produced a more integrated picture by estimating total assimilation during the month of July, assuming that each tree's photosynthetic light-response curve remains constant (Fig. S5). While trees in shaded bicultures had lower estimated assimilation than in monoculture in two of our focal species (*B. papyrifera* and *A. rubrum*), those in twelve-species plots had similar assimilation compared to those in monoculture in all four species. It may be that the intermediate light environment in these twelve-species plots allowed trees to avoid photoinhibition without becoming frequently light-limited (Fig. S2). We caution that these measurements are only based on top leaves, such that we cannot directly evaluate whole-plant carbon gain.

These estimates of assimilation during July cannot explain certain features in our stem growth data—including, for instance, the clearly positive effect of neighbor size on growth in *T. americana*. We next discuss two kinds of phenomena that could contribute to variation in growth rates, but which analyses based on light-response curves do not account for: Delayed senescence and microclimatic effects. Both may contribute to potential positive effects of shading by neighbors.

T. americana in shaded biculture dropped its leaves nearly a month later into the fall compared to monoculture (Fig. 6). We also found accelerated senescence in full sun in *A. rubrum*. Given that most leaves remained photosynthetically active until shortly before abscission (as in Mattila et al. 2018), shade could allow these trees a longer period of carbon gain. The pattern that the light environment affects senescence timing admits at least two explanations: (1) that plants in the sun accumulate phenological cues for senescence related to temperature, or (2) that excess light and other stresses cause damage that

accelerates senescence (Cavender-Bares et al. 2000; Brelsford et al. 2019), especially as the temperature declines, rendering leaves more susceptible to photodamage (Juvany et al. 2013; Renner & Zohner 2019). Contrary to the first explanation, air temperatures in full sun remained higher than in shaded plots.

Although we emphasize the role of light stress, other microclimatic factors could contribute to variation in photosynthetic rates among treatments. Because we aimed to control the chamber microclimate, our light-response curves may not capture the influence of the ambient microclimate. For example, Ψ_{PD} was slightly more negative in shaded bicultures, while Ψ_{MD} was more negative in monocultures. These results are consistent with the idea that soil moisture is higher in monocultures, as we found, while daytime VPD is higher in high biomass plots, as Wright et al. (2018) found on hot, dry days at Cedar Creek. Our water potential measurements show that water stress was not very severe in any treatment, but even modest differences could change the timing of stomatal closure (Brodribb et al. 2003). It also seems plausible that greater light exposure may make leaf temperature higher in monoculture (Schymanski et al. 2013), which could push leaves above thermal optima for photosynthesis.

In summary, we contend that being shaded has both costs and benefits. Shade reduces the light available for photosynthesis, but it may also prevent chronic stress caused by excess light, allowing the plant to use the light it absorbs more efficiently. Both factors must be considered together in order to show whether shade helps or harms a plant.

Mechanisms of photoprotection

Plants' strategies to avoid damage from excess light can be classified broadly into biochemical and structural strategies. We show that trees in full sun allocate more to biochemical photoprotection, as shown by lower PRI and higher qN in most species. The two most shade-tolerant species—*A. negundo* and *T. americana*—show no greater capacity for non-photochemical quenching when grown in full sun than in shade. Across a gradient of shade to sun, these species may experience large increases in $\square_{NO}$, and may suffer from greater photodamage as a result, as supported by patterns of dark-acclimated F_v/F_m. This

result is consistent with other research that finds that shade-adapted species often fail to increase their photoprotective abilities in the sun (Montgomery et al. 2008).

Our leaf angle survey is also consistent with the idea that plants may steeply incline their leaves to avoid intercepting excess light—a form of structural photoprotection. Leaves that are steeply inclined intercept less light per unit area, particularly during midday, when solar radiation is otherwise most intense. The dramatic trend in leaf angles suggests that these species use gross structural characteristics to partially regulate their light absorption.

Plants—especially those adapted to the shade—may lack perfect photoprotective mechanisms in part because they are costly. Building pigments and proteins for photoprotection uses nutrients that could otherwise be allocated to chlorophyll, RuBisCO, or structural tissue components. Furthermore, slow relaxation of NPQ may hinder photosynthesis even when light declines enough to relieve the imminent threat of damage (Zhu et al. 2004; Murchie & Niyogi 2011; Kromdijk et al. 2016). Steep leaf angles may also decrease carbon assimilation by reducing light interception even when light is limiting. All the same, plants in full sun may need these mechanisms to avoid even greater costs caused by photodamage. That most species upregulate photoprotection in high light, despite the costs, implies that these species may otherwise incur a risk of damage from excess light. These findings reinforce our conclusion that light stress shapes species interactions.

The case for facilitation

We found that shade from large neighbors increases both net photosynthetic rates and stem growth rates in shade-tolerant species. This finding has precedents: Ball et al. (1991) and Egerton et al. (2000) showed that shade enhances photosynthesis and growth of evergreen *Eucalyptus* seedlings during the winter, when cold imposes a risk of photoinhibition. Howell et al. (2002) also found that among the evergreen divaricating shrubs of New Zealand, leafless outer branches reduce photoinhibition during the winter by shading inner leaves. Species can also facilitate each other from light stress in communities of phytoplankton (Gerla et al. 2011), which nearly all face some risk of photoinhibition (Edwards et al.

2015), especially under cold temperatures (Edwards et al. 2016) These studies show that facilitation through shading can occur in many kinds of environments, but perhaps more so in stressful ones.

Much of the work on facilitation in plant communities is guided by the stress-gradient hypothesis (SGH), which proposes that facilitative interactions are more common in stressful environments (Bertness & Callaway 1994; Maestre et al. 2009). We can understand photoinhibition in light of the SGH as follows: Stressful conditions limit the use of light for photochemistry, turning high light exposure into an additional stressor. Under such conditions, shade from neighbors can ameliorate stress, resulting in facilitation. Under benign conditions, where plants can use more of the available light for photochemistry, high light exposure may not cause damage. Here, shading by neighbors can cause light limitation, resulting in an adverse, competitive effect on growth. As we show here, whether or not a species is stressed by its environment also depends on its own physiological tolerances.

Competition and facilitation in biodiversity-ecosystem function relationships

The SGH brought attention to facilitation in plant ecology, including in biodiversity-ecosystem function research. For example, Mulder et al. (2001) showed that in experimental moss communities, biodiversity increased productivity only under drought, as species interactions became more positive. But facilitation is still overlooked in biodiversity-ecosystem function research (Wright et al. 2017)—and with some exceptions (e.g. Wright et al. 2015), even studies that do invoke facilitation seldom seek to explain how and why it actually occurs, and how it contributes to the overall effect of diversity.

Overyielding—or biodiversity-enhanced growth—is a hallmark of positive biodiversity-ecosystem function relationships. A whole community can only overyield if at least one of its constituent species overyields. Even though we test how species growth changes with neighbor size, not neighbor diversity, our results show that shading allows some species to grow faster in shaded bicultures or twelve-species plots. In the same experiment, Grossman et al. (2017) found that *T. americana* had the greatest overyielding in multi-species plots of any broadleaf species, especially when growing with conifers or *B.*

papyrifera. Grossman et al. (2017) further showed that conifer partners in these species combinations also grew faster than they did in monoculture, resulting in community overyielding.

The two broadleaf species that were facilitated by shade had low tolerance to excess light, and likely benefited from the milder microclimate their larger neighbors created. The conifer species, which are fast-growing and less shade-tolerant (except for *P. strobus*), may also have grown faster in bicultures with broadleaf species because they faced less competition for light than in monoculture. Other researchers have found that heterogeneity in shade tolerance explains the effect of tree diversity on productivity, but attributed this result to higher stand-level light capture enabled by crown complementarity (Zhang et al. 2012; Toïgo et al. 2017; Searle and Chen 2019). We show that facilitation of shade-tolerant species by shade-intolerant species is an equally compelling explanation.

We can place these findings in the context of the three classes of facilitative mechanisms distinguished by Wright et al. (2017):

1. Biotic facilitation, which is mediated by higher-order trophic interactions, such as promotion of shared mutualists or dilution of natural enemy loads;
2. Resource enrichment, in which some species increase resource availability for others; and,
3. Stress amelioration, in which some species create a favorable microclimate for others.

In the FAB experiment, diversity has a small and variable effect on damage by aboveground herbivores and pathogens, which suggests that enemy-mediated biotic facilitation may have a limited role (Grossman et al. 2018). Nutrient enrichment is probably not a major mechanism for facilitation here because, although nitrogen is the main limiting mineral nutrient at Cedar Creek (Tilman 1987), none of the planted tree species associates with nitrogen-fixing microbes. What remains is stress amelioration, which is likely to be the main kind of facilitation in this experiment, perhaps acting in concert with niche partitioning to explain the complementarity effect.

In the literature on biodiversity and ecosystem function, the attempt to parse out explanations—such as niche partitioning and facilitation—often depends on ever-finer statistical partitions of biomass or productivity data (Loreau & Hector 2001; Fox & Kerr 2012), whose interpretation is often debated

(Carroll et al. 2011; Pillai et al. 2019). But because productivity has physiological causes, we can explain patterns in productivity using physiological measurements. These techniques can help us determine what specific kinds of interactions among plants and their environment produce biodiversity-productivity relationships, and how these interactions emerge from basic aspects of plant function.

In this study, survey-based tree growth data and physiological measurements both show that certain species respond positively and others respond negatively to the size of their neighbors. But only the physiological measurements allow us to explain why these species diverge—they show that these interactions emerge in part from the photosynthetic responses of trees to the light environment created by their neighbors. The insights gained from measuring physiological mechanisms may benefit community ecology more widely.

Acknowledgements

University of Minnesota, including Cedar Creek ESR, lies on the ancestral, traditional, and contemporary Land of the Dakota. Conversations with Jake Grossman and Laura Williams inspired much of this research. Beth Fallon, German Vargas G., Artur Stefanski, Daniel Stanton, and Danielle Way all gave valuable advice about measuring photosynthesis. We are indebted to Cathleen Nguyen, Chris Buyarski, Troy Mielke, Kally Worm, Jim Krueger, Pam Barnes, Mark Saxhaug, and Dan Bahauddin for making research in FAB possible. Sarah Hobbie and Peter Reich helped design the FAB experiment, and countless Cedar Creek interns have taken part in the stem growth survey. The Cavender-Bares lab (especially Jake Grossman and Gerard Sapès), Daniel Stanton, German Vargas G., Artur Stefanski, Jamie Mosel, José Lopez, and David Kramer all provided feedback on the results or manuscript. Morgan Tingley made a useful suggestion about the title. FAB is maintained with support from National Science Foundation under DEB #1234162 to Cedar Creek LTER. Spectral measurements were conducted as part of NSF/NASA DEB #1342778 to J.C.B. and R.M.. S.K. has been supported by an NSF Graduate Research Fellowship (Grant No. 00039202) and a UMN Doctoral Dissertation Fellowship. R.M. is also supported by Minnesota Agricultural Experiment Station project MIN-42-060.

References

Ammer C. Diversity and forest productivity in a changing climate. New Phytologist 221, 50–66 (2019).

Ball MC, Hodges VS, Laughlin GP. Cold-Induced Photoinhibition Limits Regeneration of Snow Gum at Tree-Line. Functional Ecology 5, 663–668 (1991).

Barry KE, Mommer L, van Ruijven J, Wirth C, Wright AJ, Bai Y, Connolly J, De Deyn G, de Kroon H, Isbell F et al. The Future of Complementarity: Disentangling Causes from Consequences. Trends in Ecology & Evolution 34: 167–180 (2019).

Bertness MD, Callaway R. Positive interactions in communities. Trends in Ecology & Evolution 9, 191–193 (1994).

Björkman O, Powles SB. Inhibition of photosynthetic reactions under water stress: interaction with light level. Planta 161, 490–504 (1984).

Braun EL. Deciduous Forests of Eastern North America. Philadelphia: Blakiston (1950).

Braun-Blanquet J. Plant Sociology (trans. Fuller GD, Conard HS). New York: McGraw-Hill (1932).

Brelsford CC, Trasser M, Paris T, Hartikainen SM, Robson TM. Understory light quality affects leaf pigments and leaf phenology in different plant functional types. biorXiv (2019). DOI: 10.1101/829036.

Brodribb TJ, Holbrook NM, Edwards EJ, Gutiérrez MV. Relations between stomatal closure, leaf turgor and xylem vulnerability in eight tropical dry forest trees. Plant, Cell & Environment 26, 443–450 (2003).

Canham CD, Finzi AC, Pacala SW, Burbank DH. Causes and consequences of resource heterogeneity in forests: interspecific variation in light transmission by canopy trees. Can. J. For. Res. 24, 337–349 (1994).

Carroll IT, Cardinale BJ, Nisbet RM. Niche and fitness differences relate the maintenance of diversity to ecosystem function. Ecology 92, 1157–1165 (2011).

Cavender-Bares J. Chilling and freezing stress in live oaks (Quercus section Virentes): Intra- and interspecific variation in PS II sensitivity corresponds to latitude of origin. Photosynthesis Research 94, 437–453 (2007).

Cavender-Bares J, Bazzaz FA. From Leaves to Ecosystems: Assessing Photosynthesis and Plant Function in Ecological Studies. In Papageorgiou GC and Govindjee (Eds.), Chlorophyll fluorescence: A Signature of Photosynthesis (pp. 737–755). Dordrecht, Netherlands: Kluwer Academic Publishers (2004).

Cavender□Bares J, Potts M, Zacharias E, Bazzaz FA. Consequences of CO2 and light interactions for leaf phenology, growth, and senescence in Quercus rubra. Global Change Biology 6, 877–887 (2000).

Demmig-Adams B, Adams, WW III. Photoprotection and Other Responses of Plants to High Light Stress. Annual Review of Plant Physiology and Plant Molecular Biology 43, 599–626 (1992).

Dybzinski R, Tilman D. Resource Use Patterns Predict Long□Term Outcomes of Plant Competition for Nutrients and Light. The American Naturalist 170, 305–318 (2007).

Edwards KF, Thomas MK, Klausmeier CA, Litchman E. Light and growth in marine phytoplankton: allometric, taxonomic, and environmental variation. Limnology and Ocenography 60, 540–552 (2015).

Edwards KF, Thomas MK, Klausmeier CA, Litchman E. Phytoplankton growth and the interaction of light and temperature: A synthesis at the species and community level. Limnology and Oceanography 61, 1232–1244 (2016).

Egerton JJG, Banks JCG, Gibson A, Cunningham RB, Ball MC. Facilitation of Seedling Establishment: Reduction in Irradiance Enhances Winter Growth of *Eucalyptus pauciflora*. Ecology 81, 1437–1449 (2000).

Ehleringer J, Werk KS. Modifications of solar radiation absorption patterns and the implications for carbon gain at the leaf level. In T. Givnish (ed.), On the Economy of Plant Form and Function. Cambridge Univ. Press, London. 57-82 (1986).

Farquhar GD, von Caemmerer S, Berry JA. A biochemical model of photosynthetic CO_2 assimilation in leaves of C_3 species. Planta 149, 78–90 (1980).

Fichtner A, Härdtle W, Li Y, Bruelheide H, Kunz M, von Oheimb G. From competition to facilitation: how tree species respond to neighbourhood diversity. Ecology Letters 20, 892–900 (2017).

Fox JW, Kerr B. Analyzing the effects of species gain and loss on ecosystem function using the extended Price equation partition. Oikos 121, 290–298 (2012).

Gamfeldt L, Snäll T, Bagchi T, Jonsson M, Gustafsson L, Kjellander P, Ruiz-Jaen MC, Fröberg M, Stendahl J, Philipson CD et al. Higher levels of multiple ecosystem services are found in forests with more tree species. Nature Communications 4, 1340 (2013).

Gamon JA, Peñuelas J, Field CB. A narrow-waveband spectral index that tracks diurnal changes in photosynthetic efficiency. Remote Sensing of Environment 41, 35–44 (1992).

Gerla DJ, Mooij WM, Huisman J. Photoinhibition and the assembly of light□limited phytoplankton communities. Oikos 120, 359–368 (2011).

Gitelson AA, Gamon JA, Solovchenko, A. Multiple drivers of seasonal change in PRI: Implications for photosynthesis 1. Leaf level. Remote Sensing of Environment 191, 110–116 (2017).

Grossman JJ, Cavender-Bares J, Hobbie SE, Reich PB, Montgomery RA. Species richness and traits predict overyielding in stem growth in an early-successional tree diversity experiment. Ecology 98, 2601–2614 (2017).

Grossman JJ, Cavender□Bares J, Reich PB, Montgomery RA, Hobbie SE. Neighborhood diversity simultaneously increased and decreased susceptibility to contrasting herbivores in an early stage forest diversity experiment. Journal of Ecology 107, 1492–1505 (2019).

Grossman JJ, Vanhellemont M, Barsoum N, Bauhus J, Bruelheide H, Castagneyrol B, Cavender-Bares J, Eisenhauer N, Ferlian O, Gravel D et al. Synthesis and future research directions linking tree diversity to growth, survival, and damage in a global network of tree diversity experiments. Environmental and Experimental Botany 152, 68–89 (2018).

Hoffmann WA, Poorter H. Avoiding Bias in Calculations of Relative Growth Rate. Annals of Botany 90, 37 (2002).

Howell CJ, Kelly D, Turnbull MH. Moa ghosts exorcised? New Zealand's divaricate shrubs avoid photoinhibition. Functional Ecology 16, 232–240 (2002).

Huang Y, Chen Y, Castro-Izaguirre N, Baruffol M, Brezzi M, Lang A, Li Y, Härdtle W, von Oheimb G, Yang V et al. Impacts of species richness on productivity in a large-scale subtropical forest experiment. Science 362, 80–83 (2018).

Juvany M, Müller M, Munné-Bosch S. Photo-oxidative stress in emerging and senescing leaves: a mirror image? J Exp Bot 64, 3087–3098 (2013).

Kothari S, Cavender-Bares J, Bitan K, Verhoeven AS, Wang R, Montgomery RA, Gamon J. Community-wide consequences of variation in photoprotective physiology among prairie plants. Photosynthetica 56, 455–467 (2018).

Kramer DM, Johnson G, Kiirats O, Edwards GE. New Fluorescence Parameters for the Determination of QA Redox State and Excitation Energy Fluxes. Photosynthesis Research 79, 209–218 (2004).

Kromdijk J, Głowacka K, Leonelli L, Gabilly ST, Iwai M, Niyogi KK, Long SP. Improving photosynthesis and crop productivity by accelerating recovery from photoprotection. Science 354, 857–861 (2016).

Külheim C, Ågren J, Jansson S. Rapid Regulation of Light Harvesting and Plant Fitness in the Field. Science 297, 91–93 (2002).

Liang J, Crowther TW, Picard N, Wiser S, Zhou M, Alberti G, Schulze E-D, McGuire AD, Bozzato F, Pretzsch H et al. Positive biodiversity-productivity relationship predominant in global forests. Science 354, aaf8957 (2016).

Lobo FA, de Barros MP, Dalmagro HJ, Dalmolin ÂC, Pereira WE, de Souza ÉC, Vourlitis GL, Rodríguez Ortíz CE. Fitting net photosynthetic light-response curves with Microsoft Excel — a critical look at the models. Photosynthetica 51, 445–456 (2013).

Long SP, Humphries S, Falkowski PG. Photoinhibition of Photosynthesis in Nature. Annual Review of Plant Physiology and Plant Molecular Biology 45, 633-62 (1994).

Loreau M, Hector A. Partitioning selection and complementarity in biodiversity experiments. Nature 412, 72–76 (2001).

Lovelock CE, Clough BF. Influence of solar radiation and leaf angle on leaf xanthophyll concentrations in mangroves. Oecologia 91, 518–525 (1992).

Maestre FT, Callaway RM, Valladares F, Lortie CJ. Refining the stress-gradient hypothesis for competition and facilitation in plant communities. Journal of Ecology 97, 199–205 (2009).

Mattila H, Valev D, Havurinne V, Khorobrykh S, Virtanen O, Antinluoma M, Mishra KB, Tyystjärvi E. Degradation of chlorophyll and synthesis of flavonols during autumn senescence—the story told by individual leaves. AoB Plants 10, ply028 (2018).

Monsi M, Saeki T. On the Factor Light in Plant Communities and its Importance for Matter Production. Ann Bot 95, 549–567 (2005).

Monteith JL, Moss CJ, Cooke GW, Pirie NW, Bell GDH. Climate and the efficiency of crop production in Britain. Philosophical Transactions of the Royal Society of London B: Biological Sciences 281, 277–294 (1977).

Montgomery RA, Goldstein G, Givnish TJ. Photoprotection of PSII in Hawaiian lobeliads from diverse light environments. Functional Plant Biology 35, 595–605 (2008).

Montgomery RA, Reich PB, Palik BJ. Untangling positive and negative biotic interactions: views from above and below ground in a forest ecosystem. Ecology 91, 3641–3655 (2010).

Mulder CPH, Uliassi DD, Doak DF. Physical stress and diversity-productivity relationships: The role of positive interactions. PNAS 98: 6704–8 (2001).

Murchie EH, Niyogi KK. Manipulation of Photoprotection to Improve Plant Photosynthesis. Plant Physiology 155, 86–92 (2011).

Niinemets Ü, Valladares F. Tolerance to Shade, Drought, and Waterlogging of Temperate Northern Hemisphere Trees and Shrubs. Ecological Monographs 76, 521–547 (2006).

Oehri J, Schmid B, Schaepman-Strub G, Niklaus PA. Biodiversity promotes primary productivity and growing season lengthening at the landscape scale. PNAS 114, 10160–10165 (2017).

Parent S, Messier C. A simple and efficient method to estimate microsite light availability under a forest canopy. Can. J. For. Res. 26, 151–154 (1996).

Pastenes C, Porter V, Baginsky C, Horton P, González J. Paraheliotropism can protect water-stressed bean (Phaseolus vulgaris L.) plants against photoinhibition. Journal of Plant Physiology 161, 1315–1323 (2004).

Pearcy RW, Muraoka H, Valladares F. Crown architecture in sun and shade environments: assessing function and trade-offs with a three-dimensional simulation model. New Phytologist 166, 791–800 (2005).

Pillai P, Gouhier TC. Not even wrong: the spurious measurement of biodiversity's effects on ecosystem functioning. Ecology 100, e02645 (2019).

Poorter H, Niinemets Ü, Ntagkas N, Siebenkäs A, Mäenpää M, Matsubara S, Pons TL. A meta-analysis of plant responses to light intensity for 70 traits ranging from molecules to whole plant performance. New Phytologist 223, 1073–1105 (2019).

Posada JM, Lechowicz M, Kitajima K. Optimal photosynthetic use of light by tropical tree crowns achieved by adjustment of individual leaf angles and nitrogen content. Annals of Botany 103, 795–805 (2009).

Potvin C, Gotelli NJ. Biodiversity enhances individual performance but does not affect survivorship in tropical trees. Ecology Letters 11, 217–223 (2008).

Ramírez-Valiente JA, Koehler K, Cavender-Bares J. Climatic origins predict variation in photoprotective leaf pigments in response to drought and low temperatures in live oaks (Quercus series Virentes). Tree Physiology 35, 521–534 (2015).

Renner SS, Zohner CM. The occurrence of red and yellow autumn leaves explained by regional differences in insolation and temperature. New Phytologist 224, 1464–1471 (2019).

Ryser P, Eek L. Consequences of phenotypic plasticity vs. interspecific differences in leaf and root traits for acquisition of aboveground and belowground resources. American Journal of Botany 87, 402–411 (2000).

Savage, J., J. Cavender-Bares, and A. Verhoeven. Habitat generalists and wetland specialists in the genus Salix vary in their photoprotective responses to drought. Functional Plant Biology 36, 300–309 (2009).

Schall P, Lödige C, Beck M, Ammer C. Biomass allocation to roots and shoots is more sensitive to shade and drought in European beech than in Norway spruce seedlings. Forest Ecology and Management 266, 246–253 (2012).

Schymanski SJ, Or D, Zwieniecki M. Stomatal Control and Leaf Thermal and Hydraulic Capacitances under Rapid Environmental Fluctuations. PLOS ONE 8, e54231 (2013).

Searle EB, Chen HYH. Complementarity effects are strengthened by competition intensity and global environmental change in the central boreal forests of Canada. Ecology Letters 23, 79–87 (2020).

Semchenko M, Lepik M, Götzenberger L, Zobel K. Positive effect of shade on plant growth: amelioration of stress or active regulation of growth rate? Journal of Ecology 100, 459–466 (2012).

Simonsohn U. Two Lines: A Valid Alternative to the Invalid Testing of U-Shaped Relationships With Quadratic Regressions. Advances in Methods and Practices in Psychological Science 1, 538–555 (2018).

Tilman D. Secondary Succession and the Pattern of Plant Dominance Along Experimental Nitrogen Gradients. Ecological Monographs 57, 189–214 (1987).

Tilman D, Isbell F, Cowles JM. Biodiversity and Ecosystem Functioning. Annual Review of Ecology, Evolution, and Systematics 45, 471–493 (2014).

Tobner CM, Paquette A, Gravel D, Reich PB, Williams LJ, Messier C. Functional identity is the main driver of diversity effects in young tree communities. Ecology Letters 19, 638–647 (2016).

Toïgo M, Perot T, Courbaud B, Castagneyrol B, Gégout J-C, Longuetaud F, Jactel H, Vallet P. Difference in shade tolerance drives the mixture effect on oak productivity. Journal of Ecology 106: 1073–1082 (2017).

Udo SO, Aro TO. Global PAR related to global solar radiation for central Nigeria. Agricultural and Forest Meteorology 97: 21–31 (1999).

Valiente-Banuet A, Verdú M, Valladares F, García-Fayos P. Functional and evolutionary correlations of steep leaf angles in the mexical shrubland. Oecologia 163, 25–33 (2010).

Valladares F, Pugnaire FI. Tradeoffs Between Irradiance Capture and Avoidance in Semi-arid Environments Assessed with a Crown Architecture Model. Annals of Botany 83, 459–469 (1999).

Watling JR, Robinson SA, Woodrow IE, Osmond CB. Responses of Rainforest Understorey Plants to Excess Light during Sunflecks. Australian Journal of Plant Physiology 24, 17–25 (1997).

Werner C, Correia O, Beyschlag W. Two different strategies of Mediterranean macchia plants to avoid photoinhibitory damage by excessive radiation levels during summer drought. Acta Oecologica 20, 15–23 (1999).

Williams LJ, Paquette A, Cavender-Bares J, Messier C, Reich PB. Spatial complementarity in tree crowns explains overyielding in species mixtures. Nature Ecology & Evolution 1, 0063 (2017).

Wong CYS, Gamon JA. Three causes of variation in the photochemical reflectance index (PRI) in evergreen conifers. New Phytologist 206, 187–195 (2015).

Wright A, Schnitzer SA, Reich PB. Daily environmental conditions determine the competition–facilitation balance for plant water status. Journal of Ecology 103, 648–656 (2015).

Wright AJ, Wardle DA, Callaway R, Gaxiola A. The Overlooked Role of Facilitation in Biodiversity Experiments. Trends in Ecology & Evolution 32, 383–390 (2017).

Wujeska A, Bossinger G, Tausz M. Responses of foliar antioxidative and photoprotective defence systems of trees to drought: a meta-analysis. Tree Physiology 33, 1018–1029 (2013).

Zemp DC, Gérard A, Hölscher D, Ammer C, Irawan B, Sundawati L, Teuscher M, Kreft H. Tree performance in a biodiversity enrichment experiment in an oil palm landscape. Journal of Applied Ecology 56, 2340–2352 (2019).

Zhang Y, Chen HYH, Reich PB. Forest productivity increases with evenness, species richness and trait variation: a global meta analysis. Journal of Ecology 100: 742–749 (2012).

Zhu X-G, Ort DR, Whitmarsh J, Long SP. The slow reversibility of photosystem II thermal energy dissipation on transfer from high to low light may cause large losses in carbon gain by crop canopies: a theoretical analysis. J Exp Bot 55, 1167–1175 (2004).

Tables

Table 1: Characteristics of species in FAB. Except for *B. papyrifera*, broadleaf species tended to grow slower than needleleaf conifers. Shade tolerance is drawn from Niinemets and Valladares (2006), who evaluated it along a 1-5 scale where higher values indicate an ability to grow under lower light.

Scientific name	Species code	Common name	Family	Leaf form	Mean RGR in monoculture, 2013-6 (/year)	Shade tolerance	Partner in shaded biculture
Acer negundo	ACNE	Box elder	Sapindaceae	Broadleaf	0.039	3.47	None
Acer rubrum	ACRU	Red maple	Sapindaceae	Broadleaf	0.379	3.44	*Pinus banksiana*
Betula papyrifera	BEPA	Paper birch	Betulaceae	Broadleaf	1.272	1.54	*Pinus banksiana*
Juniperus virginiana	JUVI	Eastern redcedar	Cupressaceae	Needleleaf	0.975	1.28	NA
Pinus banksiana	PIBA	Jack pine	Pinaceae	Needleleaf	2.288	1.36	NA
Pinus resinosa	PIRE	Red pine	Pinaceae	Needleleaf	1.619	1.89	NA
Pinus strobus	PIST	White pine	Pinaceae	Needleleaf	1.722	3.21	NA
Quercus alba	QUAL	White oak	Fagaceae	Broadleaf	0.735	2.85	*Pinus strobus*
Quercus ellipsoidalis	QUEL	Northern pin oak	Fagaceae	Broadleaf	0.722	NA	*Pinus strobus*
Quercus macrocarpa	QUMA	Bur oak	Fagaceae	Broadleaf	0.547	2.71	*Betula papyrifera*
Quercus rubra	QURU	Northern red oak	Fagaceae	Broadleaf	0.505	2.75	*Pinus strobus*
Tilia americana	TIAM	American basswood	Tiliaceae	Broadleaf	0.724	3.98	*Pinus strobus*

Figure captions

Fig. 1, Left: When measuring carbon assimilation across light intensities for a single leaf, one usually finds a saturating curve. Consider two hypothetical photosynthetic light-response curves of leaves from unstressed (blue) and photoinhibited (red) plants, where the unstressed plant's neighbors reduce its light exposure. Given a light-response curve, a reduction in light tends to reduce photosynthesis (represented by the small black arrow along the red curve). But if a long-term reduction in light spares the plant from photoinhibition, it can change the shape of the curve such that carbon assimilation at any given light level is greater (represented by the small black vertical arrow). The balance (represented by the large dashed arrow) may either increase or reduce carbon assimilation. In this framework, shading most often helps when light is abundant: the risk of photoinhibition is greater, and the proportional cost of a given percentage decline in light is lower, since light-response curves are usually concave-down.

Right: To allow us to compare photosynthetic rates visually, we should put the two light-response curves on a common *x*-axis that represents ambient light, as in an adjacent open field. We need to scale the blue light response curve horizontally because when the stressed plant receives the amount of light corresponding to the red dashed line in (A), the unstressed plant receives a proportionally lower amount, here represented by the blue dashed line. By stretching the blue curve proportionally such that these two lines coincide, we can compare the true estimated photosynthetic rates at a given light availability.

Fig. 2: Relative growth rate (RGR) of woody stem volume in individuals of each species between fall 2016 and 2018 as a function of the total stem volume of all neighbors. Gray dots represent individuals, and the OLS regression line is fit through the individual-level data. Large colored dots are aggregated to the plot scale, as described in the main text, and color-coded by treatment. A shaded biculture is a plot in which the focal broadleaf species grows with either a conifer or *B. papyrifera* (unless *B. papyrifera* is the focal broadleaf species). An open biculture is a plot in which the focal broadleaf grows with another broadleaf species (other than *B. papyrifera*).

Fig. 3: Mass-based photosynthetic light-response curves for four broadleaf species. The left panels display photosynthetic rates as a function of chamber light intensity; the right panels represent an estimate of realized photosynthetic rates as a function of ambient light intensity, which are lower because of shading by neighbors (as in Fig. 1B). Species are arranged from the least shade-tolerant (*B. papyrifera*) to the most (*T. americana*). Error bars in left panels are ± 1 SE.

Fig. 4: Dark-acclimated F_v/F_m, qN, $\square_{NO}$, and PRI as a function of relative light availability across species and treatments. Best-fit lines come from species-specific OLS regressions.

Fig. 5: Compared to shade-intolerant species, shade-tolerant species show greater declines in dark-acclimated F_v/F_m and smaller increases in qN as light availability increases. A_{sat} derived from light-response curves correlates positively and strongly with dark-acclimated F_v/F_m; slopes are statistically indistinguishable among species.

Fig. 6: Timing of fall leaf abscission in monoculture and shaded biculture treatments of *T. americana*.

Fig. 7: Top leaf angles of *A. rubrum* (left), *Q. ellipsoidalis* (middle), and *T. americana* (right) across treatments.

Fig. S1: Example images of *Tilia americana* in shaded biculture (top) and monoculture (bottom). Red scale bars represent about 1 m in the foreground.

Fig. S2: Relative light availability (top) and specific leaf area (SLA; bottom) of each species across treatments. SLA is the reciprocal of leaf mass per area (LMA). We show SLA values from all leaves used in photosynthesis and chlorophyll fluorescence measurements. Error bars in left panels are ± 1 SE.

Fig. S3: Growth of woody stem volume in individuals of each species between fall 2017 and 2018 as a function of the total stem volume of all neighbors. Gray dots represent individuals, while colored dots are aggregated to the plot scale and color-coded by treatment. Two OLS regression lines are fit for each species: One (blue) to all data, and one (red) excluding trees that died between 2017 and 2018.

Fig. S4: Responses of ETR and stomatal conductance to light availability for the four focal broadleaf species. Error bars are ± 1 SE.

Fig. S5: An estimate of total carbon assimilation across species and treatments throughout the month of July, calculated by applying a time series of solar radiation from a nearby weather station as inputs to our ambient light-response curves. Error bars are ± 1 SE.

Fig. S6: A ternary plot depicting variation among species and treatments in $\square_{PSII}$, $\square_{NPQ}$, and $\square_{NO}$, as calculated using the lake model derivations of Kramer et al. (2004). These three quantities describe light energy dissipation through photochemistry, through non-photochemical quenching, and through non-regulated dissipation, respectively. A thick dashed line represents 0.83 the theoretical maximum efficiency of PSII posited in Tietz et al. (2017). Deviations to the lower right of this line represent increasingly high $\square_{NO}$, which can result in photodamage.

Fig. S7: Water potential before dawn (Ψ_{PD}; top) and at midday (Ψ_{MD}; bottom) as a function of light availability. Data are from monoculture and shaded biculture treatments in all eight species (Ψ_{PD}) or only the four focal species (Ψ_{MD}). Best-fit lines come from species-specific OLS regressions. Two outliers in Ψ_{PD} are not included.

Figures

Fig. 1

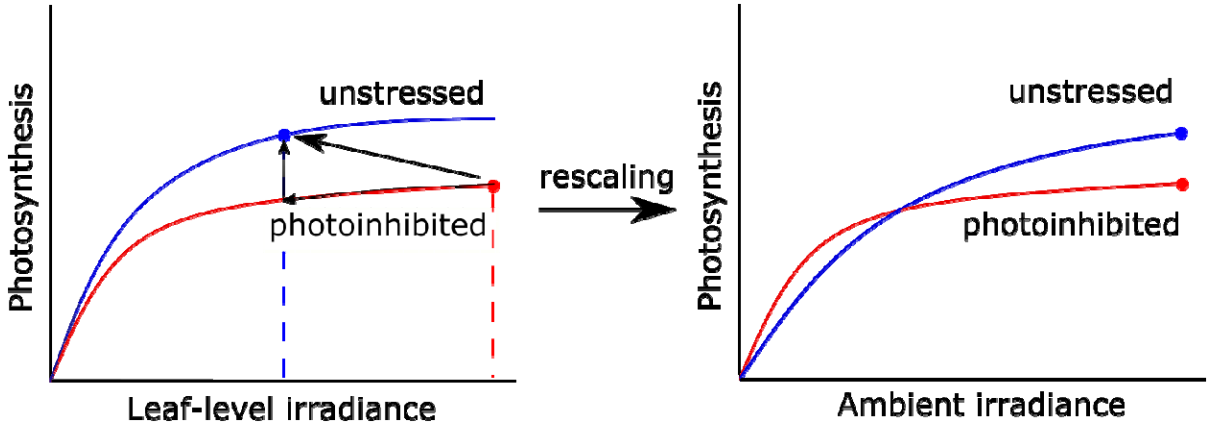

Fig. 2

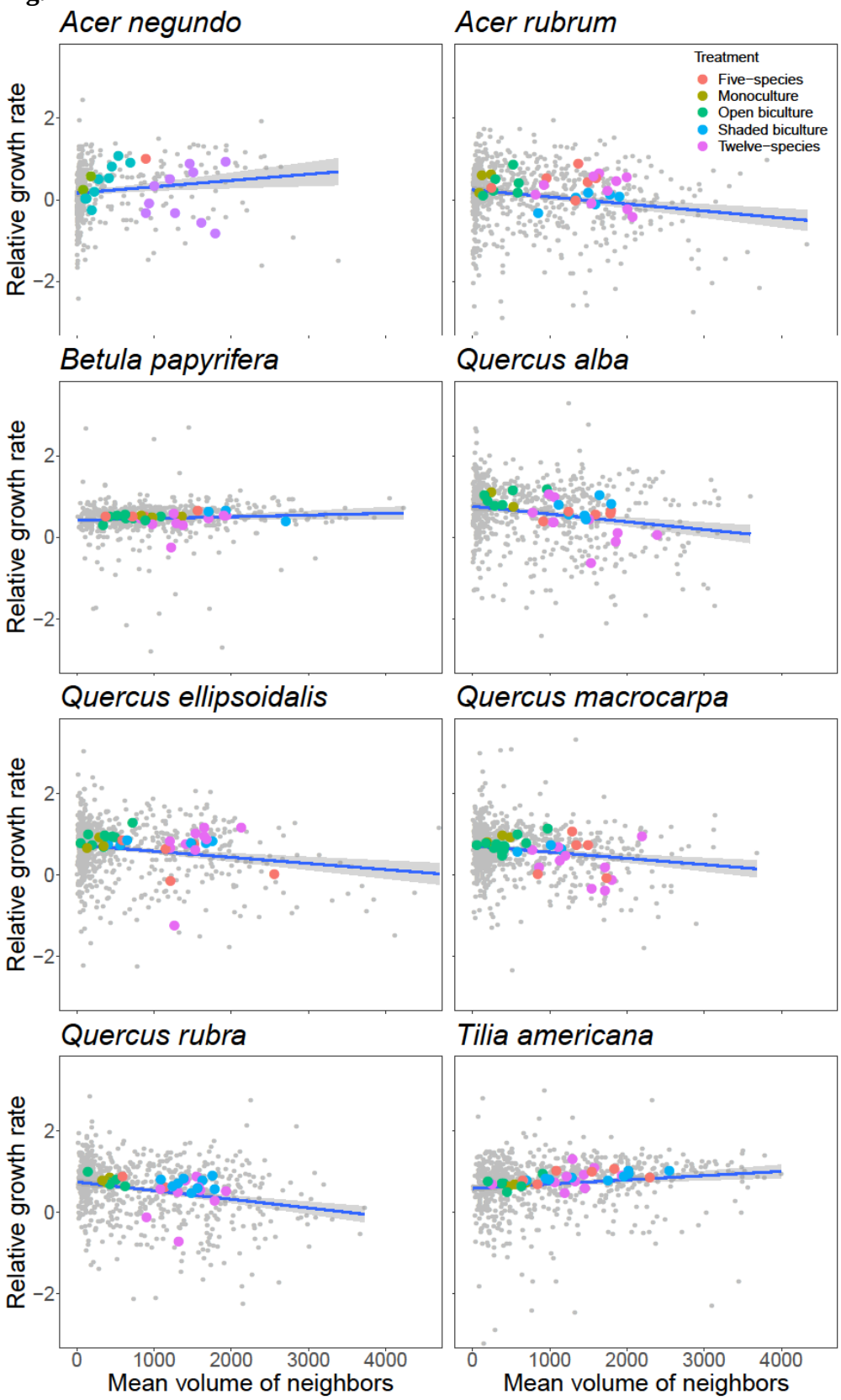
Acer negundo
Acer rubrum
Betula papyrifera
Quercus alba
Quercus ellipsoidalis
Quercus macrocarpa
Quercus rubra
Tilia americana
Treatment
Five−species
Monoculture
Open biculture
Shaded biculture
Twelve−species
Relative growth rate
2
0
−2
0
1000
2000
3000
4000
Mean volume of neighbors

Fig. 3

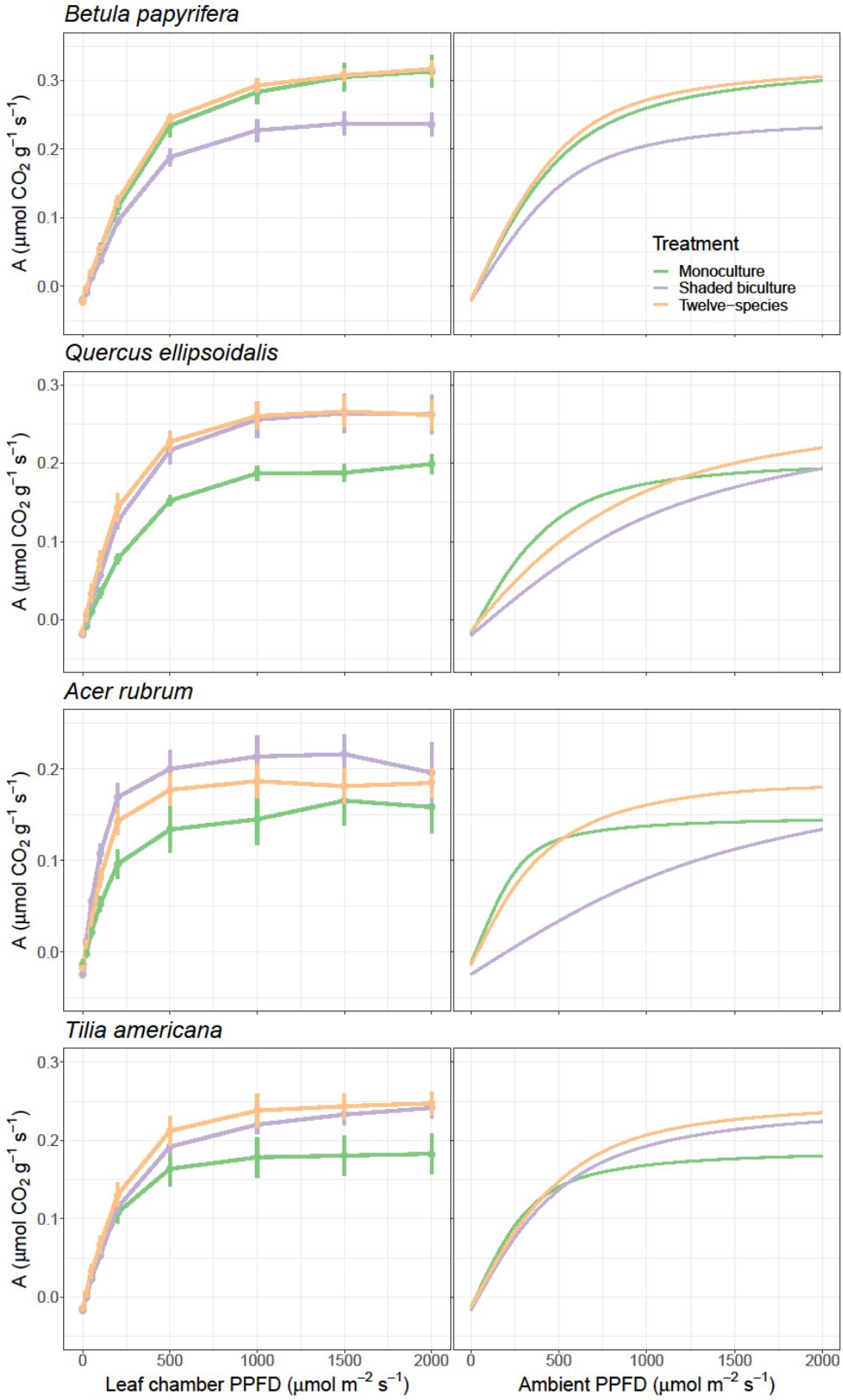
Betula papyrifera
Quercus ellipsoidalis
Acer rubrum
Tilia americana
A (µmol CO2 g−1 s−1)
0.0
0.1
0.2
0.3
Treatment
Monoculture
Shaded biculture
Twelve−species
0
500
1000
1500
2000
Leaf chamber PPFD (µmol m−2 s−1)
Ambient PPFD (µmol m−2 s−1)

Fig. 4

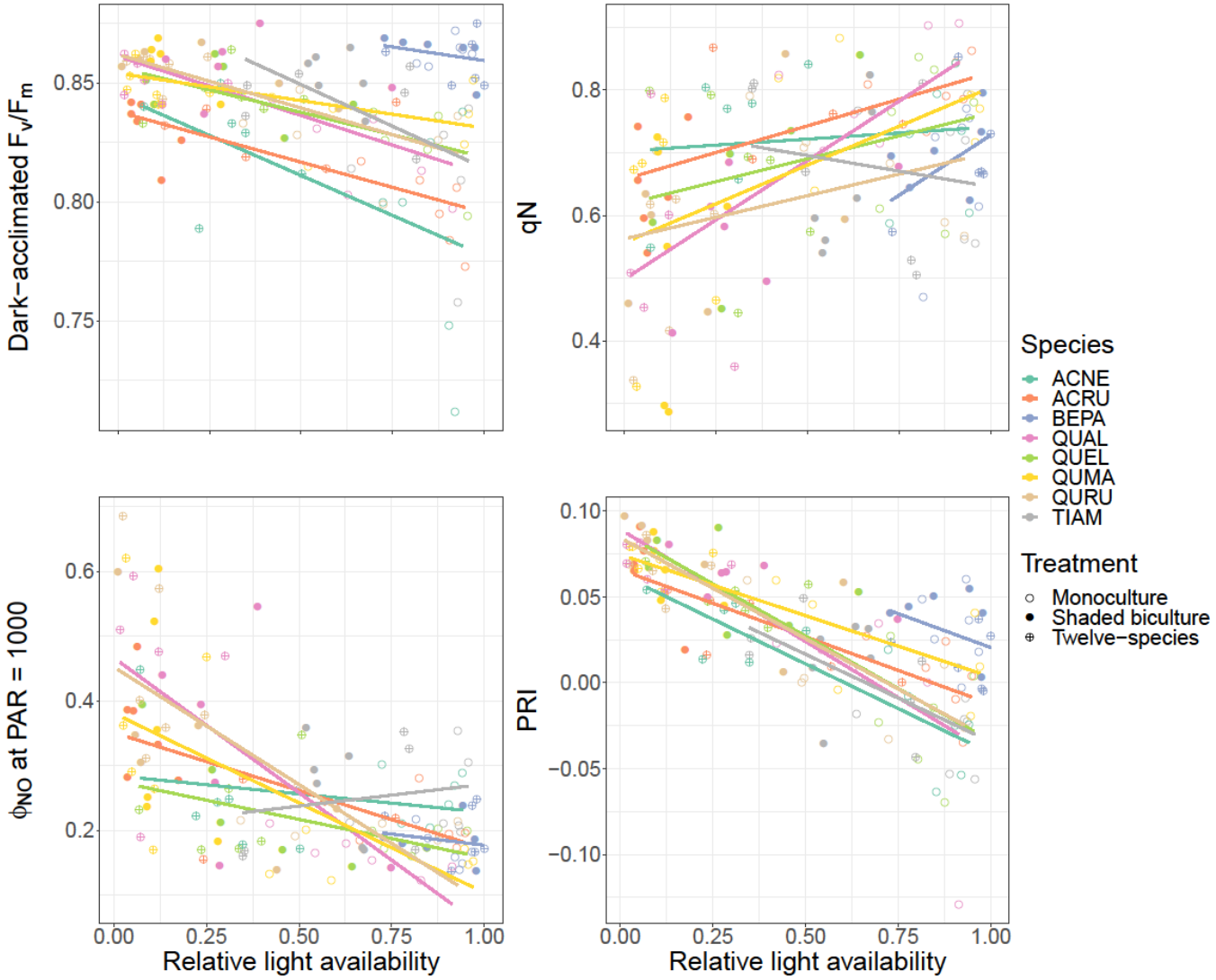
Dark−acclimated F_v/F_m
0.85
0.80
0.75
qN
0.8
0.6
0.4
ϕ_{NO} at PAR = 1000
0.6
0.4
0.2
PRI
0.10
0.05
0.00
−0.05
−0.10
0.00
0.25
0.50
0.75
1.00
Relative light availability
Species
ACNE
ACRU
BEPA
QUAL
QUEL
QUMA
QURU
TIAM
Treatment
Monoculture
Shaded biculture
Twelve−species

Fig. 5

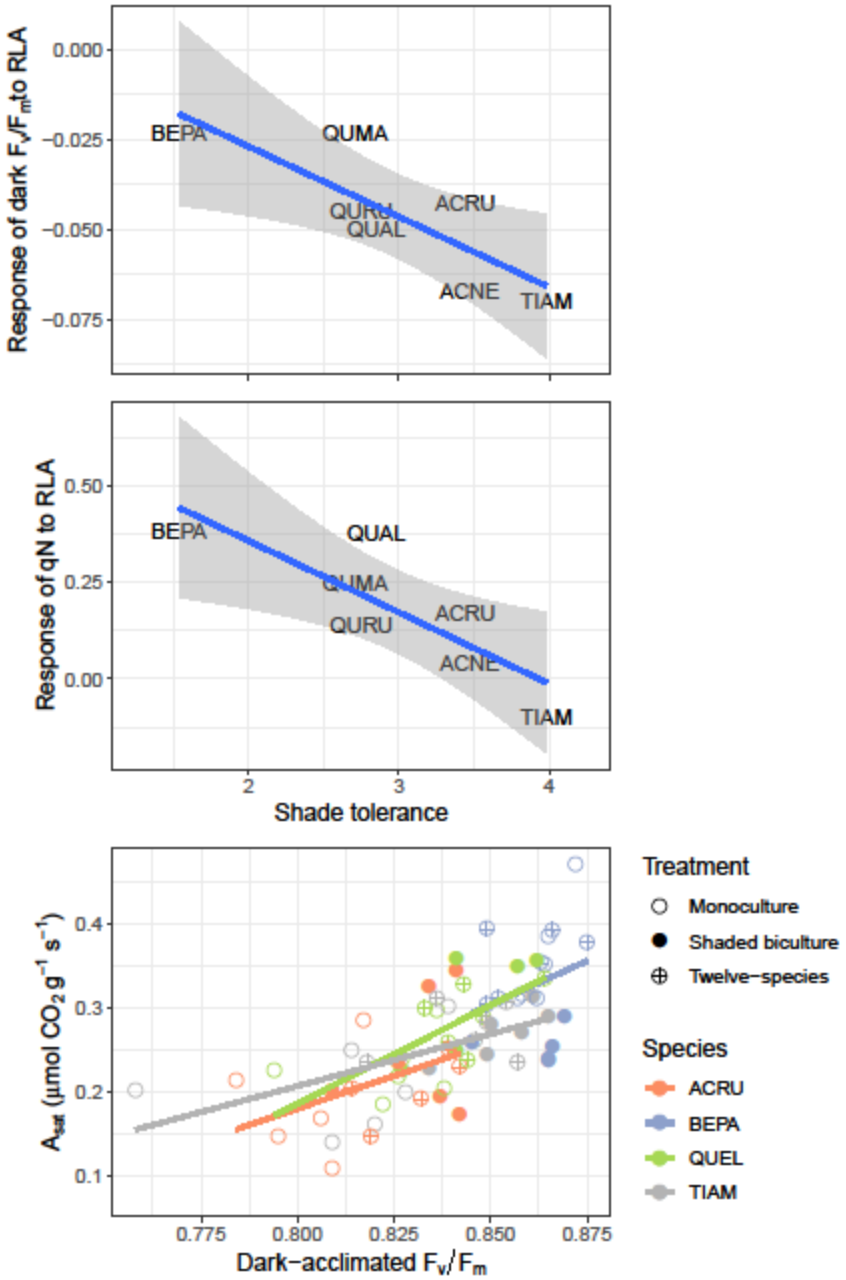
Response of dark F_v/F_m to RLA
0.000
−0.025
−0.050
−0.075
BEPA
QUMA
QURU
QUAL
ACRU
ACNE
TIAM
Response of qN to RLA
0.50
0.25
0.00
BEPA
QUAL
QUMA
QURU
ACRU
ACNE
TIAM
2
3
4
Shade tolerance
A_{sat} (µmol CO_2 g^{-1} s^{-1})
0.4
0.3
0.2
0.1
0.775
0.800
0.825
0.850
0.875
Dark−acclimated F_v/F_m
Treatment
Monoculture
Shaded biculture
Twelve−species
Species
ACRU
BEPA
QUEL
TIAM

Fig. 6

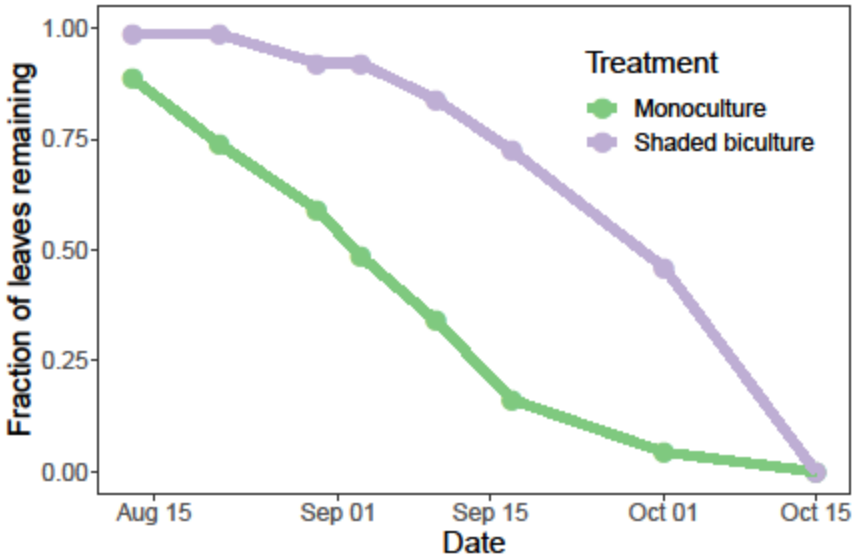
Treatment
Monoculture
Shaded biculture
Fraction of leaves remaining
1.00
0.75
0.50
0.25
0.00
Aug 15
Sep 01
Sep 15
Oct 01
Oct 15
Date

Fig. 7

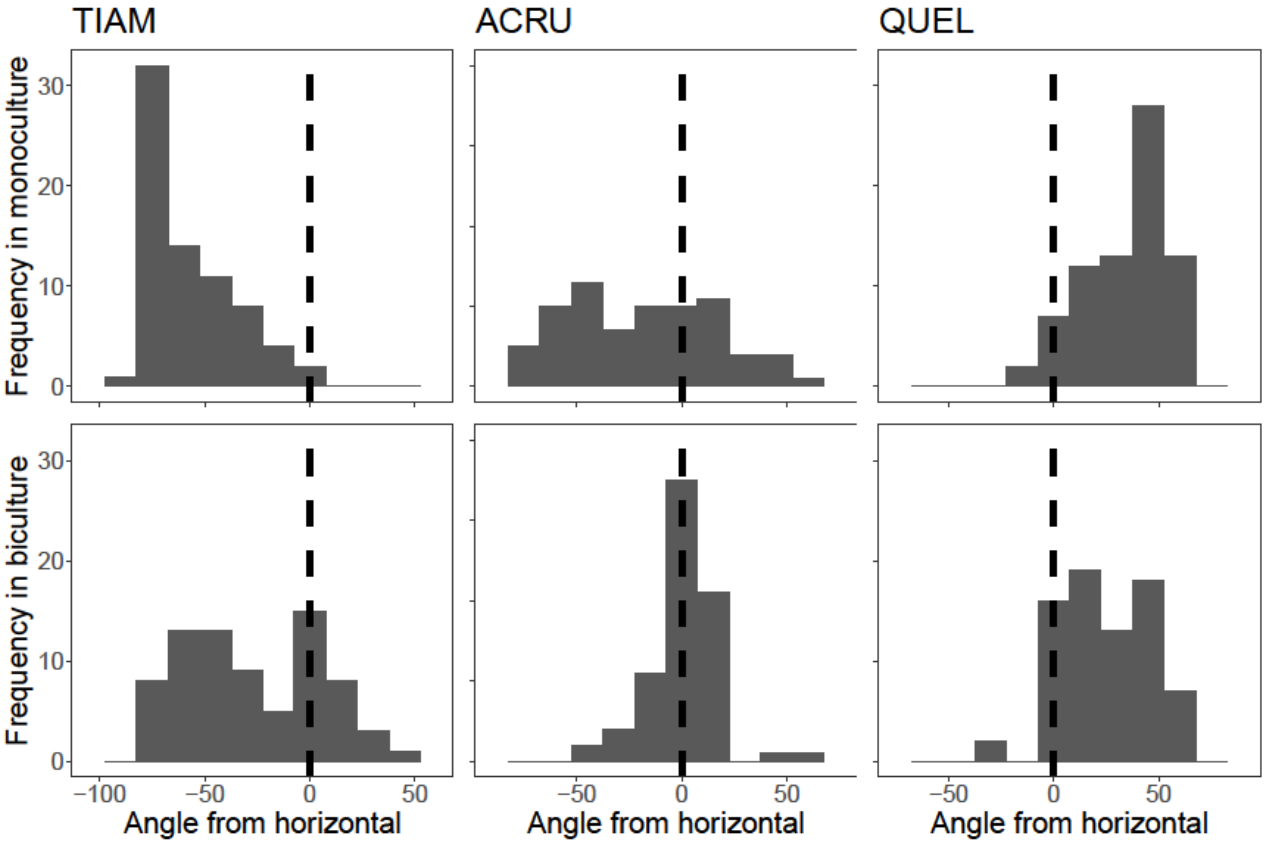
TIAM
ACRU
QUEL
Frequency in monoculture
Frequency in biculture
30
20
10
0
−100
−50
0
50
Angle from horizontal

Supplement to: "Throwing shade: Physiological responses to light mediate competition and facilitation in a tree diversity experiment"

Materials and Methods

Photosynthetic light-response curve methods

We measured photosynthetic-light response curves from the four focal species (*Acer negundo*, *Betula papyrifera*, *Quercus ellipsoidalis*, and *Tilia americana*) during July 2018 using an LI-6400 gas exchange system (LI-COR BioSciences, Lincoln, NE) with a 6400-40 Leaf Chamber Fluorometer head. From each tree (n = 72 total), we selected a fully expanded, sun-exposed leaf with no visible disease or herbivory. We noted the angle of each leaf relative to horizontal to the nearest 15˚ before beginning measurements. Each curve had nine steps in descending order of brightness: 2000, 1500, 1000, 500, 200, 100, 50, 20, and 0 µmol m^{-2} s^{-1}.

During each curve, we controlled environmental conditions to reduce the immediate effects of environmental conditions other than light on stomatal conductance. We kept relative humidity at a favorable level, typically between 65 and 75%, and set the block temperature as close as possible to 25 ˚C. The reference CO_2 concentration remained at 400±10 ppm. We kept each leaf in the chamber for at least five minutes before beginning each curve. We checked that outputs were stable, and matched IRGAs before each measurement.

Since it is hard to control chamber conditions perfectly, any differences that remain among treatments could contribute to the variation we observe in photosynthetic function. During light-response curves, we found no difference among treatments in leaf-to-air VPD within the chamber. There were significant but slight differences in leaf temperature inside the chamber; leaves in monoculture, shaded biculture, and twelve-species plots had average temperatures of 27.7 ˚C, 26.5 ˚C, and 27.0 ˚C, respectively. Previous studies on the temperature response of some of the same species in Minnesota have typically found thermal optima below 26 ˚C (Sendall et al. 2015). But while cooler leaves may be closer

to thermal optima, the small differences we find in leaf temperature cannot explain much of the variation in photosynthetic rates.

In all but five light-response curves, we also used a saturating pulse to measure light-acclimated chlorophyll fluorescence at each light level. These data allowed us to calculate ϕ_{PSII}, a measure of the efficiency of Photosystem II (PSII) at each actinic (or photosynthetic) light level, as:

$$\phi_{PSII} = \frac{F_m' - F_s}{F_m'}$$

where F_s is the steady-state fluorescence yield under actinic light, and F_m' is the maximum fluorescence yield of the actinic light-acclimated sample following a saturating light pulse, which temporarily closes all PSII reaction centers. From this parameter, we calculated electron transport rate as:

$$ETR = \phi_{PSII} \times PPFD \times 0.42 \times 0.5$$

where PPFD is photosynthetic photon flux density (the light level inside the chamber, in μmol m^{-2} s^{-1}), 0.42 is an estimate of leaf absorptance, and 0.5 is an estimate of the fraction of photons that are captured by PSII rather than PSI. Electron transport rate is a key parameter because electron transport is one of the main steps that is capable of limiting photosynthesis (Farquhar et al. 1980), especially when light availability or PSII efficiency are low.

Chlorophyll fluorescence procedure

As described in the main text, we used dark- and light-acclimated measurements of chlorophyll fluorescence to calculate several derived parameters, from which we make inferences about photosynthetic and photoprotective function. Most importantly, we wanted to assess: (1) capacity for non-photochemical quenching, as measured through the parameters qN or NPQ; and (2) the partitioning of light energy dissipation among pathways, as assessed using the quantum yields ϕ_{PSII}, ϕ_{NPQ}, and ϕ_{NO}.

These derived chlorophyll fluorescence parameters are calculated from a few basic measurements taken during the dark- and light-acclimated measurements, including: F_o, the minimum fluorescence yield of a dark-acclimated sample with all PSII reaction centers open; F_o', the minimum fluorescence yield of a

light-acclimated sample with all PSII reaction centers open (following far-red light exposure); and F_m, the maximum fluorescence yield of a dark-acclimated sample following a saturating pulse. F_v, the variable fluorescence yield of a dark-acclimated sample, is calculated as $F_m - F_o$.

The parameters qN and NPQ are meant to indicate the rate constant of the thermal dissipation of energy from PSII (Bilger and Schreiber 1986; Bilger and Björkman 1990). These parameters increase with the use of NPQ to dissipate light—in this case, under exposure to 1000 µmol m^{-2} s^{-1}. They are calculated, respectively, as:

$$qN = 1 - \frac{F_m' - F_o'}{F_m - F_o}; NPQ = \frac{F_m - F_m'}{F_m'}$$

In our dataset, qN is highly correlated (R^2 = 0.96) with the natural logarithm of NPQ; we chose to report qN to easily visualize variation among leaves with low NPQ and to help satisfy the error term normality assumption of OLS regression.

The quantum yields Φ_{PSII}, Φ_{NPQ}, and Φ_{NO} represent the proportions of absorbed light energy that are dissipated through photochemistry, non-photochemical quenching, and non-regulated dissipation. Since these pathways exhaust the options, their quantum yields sum to 1. We calculated them following the "lake model" derivation of Kramer et al. (2004), which treats photosynthetic reaction centers as connected by shared antennae. We achieve qualitatively similar results using the simpler analogues found in Hendricksen et al. (2005).

The parameter Φ_{PSII} is calculated as shown above (Supplemental Methods, *Photosynthetic light-response curve procedure*). In the derivation from Kramer et al. (2004), Φ_{NPQ} and Φ_{NO} are calculated using the parameter qL, an estimate of the fraction of open PSII reaction centers. qL is calculated as:

$$qL = \frac{F_m' - F_s}{F_m' - F_o'} \frac{F_o'}{F_s}$$

Given this parameter, we can calculate Φ_{NO} as:

$$\phi_{NO} = \frac{1}{NPQ + 1 + qL\left(\frac{F_m}{F_o} - 1\right)}$$

and given the other two quantum yields, we can calculate ϕ_{NPQ} as:

$$\phi_{NPQ} = 1 - \phi_{PSII} - \phi_{NO}$$

Many researchers, including Murchie and Lawson (2013) and Tietz et al. (2017) treat ~0.83 as a theoretical maximum of ϕ_{PSII} (or dark-acclimated F_v/F_m) after a period of dark-acclimation long enough to reduce non-photochemical quenching to zero. Similarly, one may treat ~0.83 as a theoretical maximum of $\phi_{PSII} + \phi_{NPQ}$, deviations from which indicate high ϕ_{NO}, and thus, a declining ability to regulate energy dissipation. We show this putative maximum in our ternary plot of the quantum yields (Fig. S6).

References

Bilger W, Björkman O. Role of the xanthophyll cycle in photoprotection elucidated by measurements of light-induced absorbance changes, fluorescence and photosynthesis in leaves of *Hedera canariensis*. Photosynthesis Research 25, 173–185 (1990).

Bilger W, Schreiber U. Energy-dependent quenching of dark-level chlorophyll fluorescence in intact leaves. Photosynthesis Research 10, 303–308 (1986).

Farquhar GD, von Caemmerer S, Berry JA. A biochemical model of photosynthetic CO2 assimilation in leaves of C 3 species. Planta 149, 78–90 (1980).

Hendrickson L, Förster B, Pogson BJ, Chow WS. A simple chlorophyll fluorescence parameter that correlates with the rate coefficient of photoinactivation of Photosystem II. Photosynthesis Research 84, 43–49 (2005).

Kramer DM, Johnson G, Kiirats O, Edwards GE. New Fluorescence Parameters for the Determination of QA Redox State and Excitation Energy Fluxes. Photosynthesis Research 79, 209–218 (2004).

Murchie EH, Lawson T. Chlorophyll fluorescence analysis: a guide to good practice and understanding some new applications. Journal of Experimental Botany 64, 3983–3998 (2013).

Sendall, KM, Reich PB, Zhao C, Jihua H, Wei X, Stefanski A, Rice K, Rich RL, Montgomery RA. Acclimation of photosynthetic temperature optima of temperate and boreal tree species in response to experimental forest warming. Global Change Biology 21, 1342–1357 (2015).

Tietz S, Hall CC, Cruz, JA, Kramer DM. NPQ(T): a chlorophyll fluorescence parameter for rapid estimation and imaging of non-photochemical quenching of excitons in photosystem-II-associated antenna complexes. Plant, Cell & Environment 40, 1243–1255 (2017).

Fig. S1

Fig. S3

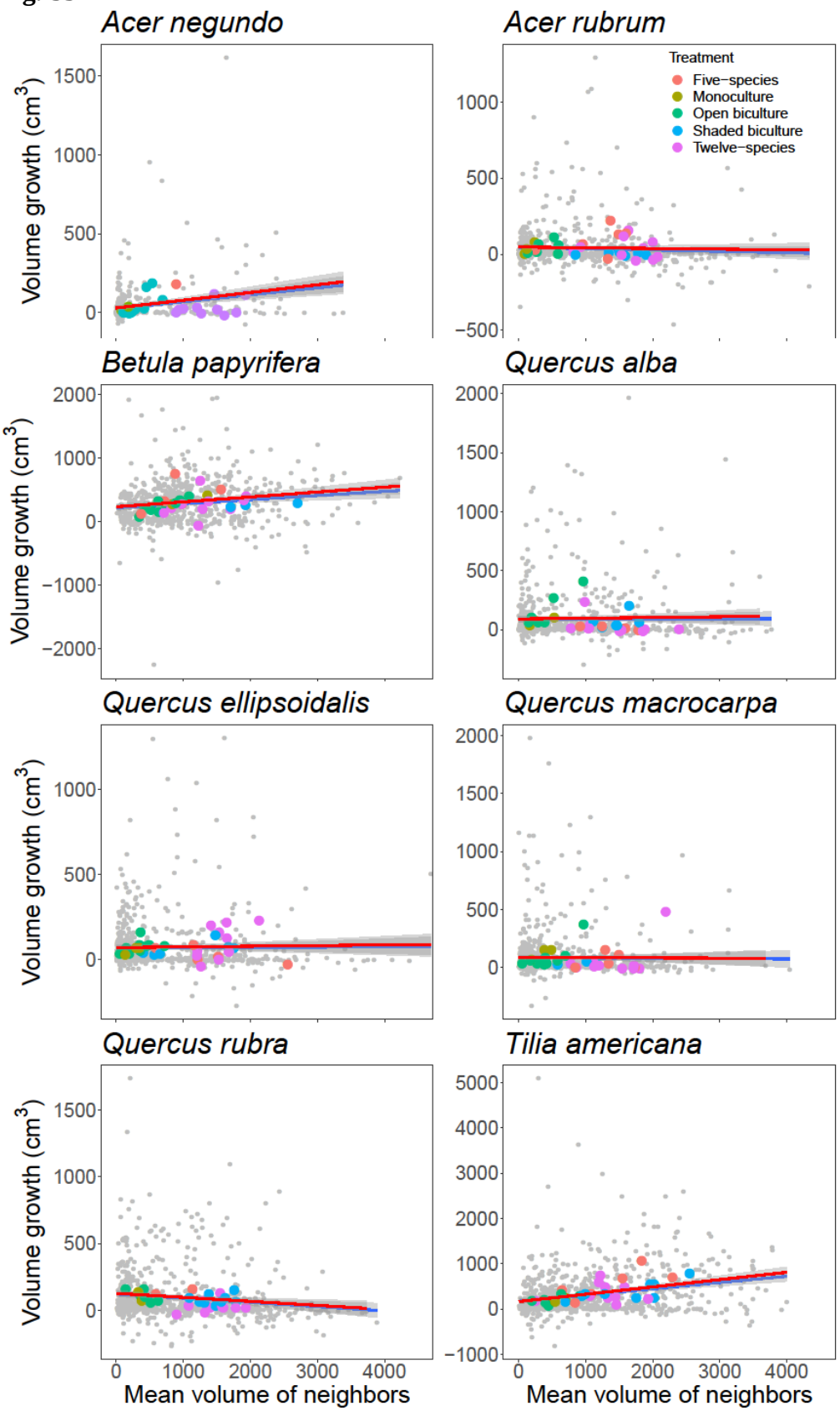
Acer negundo
Acer rubrum
Betula papyrifera
Quercus alba
Quercus ellipsoidalis
Quercus macrocarpa
Quercus rubra
Tilia americana
Treatment
Five−species
Monoculture
Open biculture
Shaded biculture
Twelve−species
Volume growth (cm3)
Mean volume of neighbors

Fig. S4

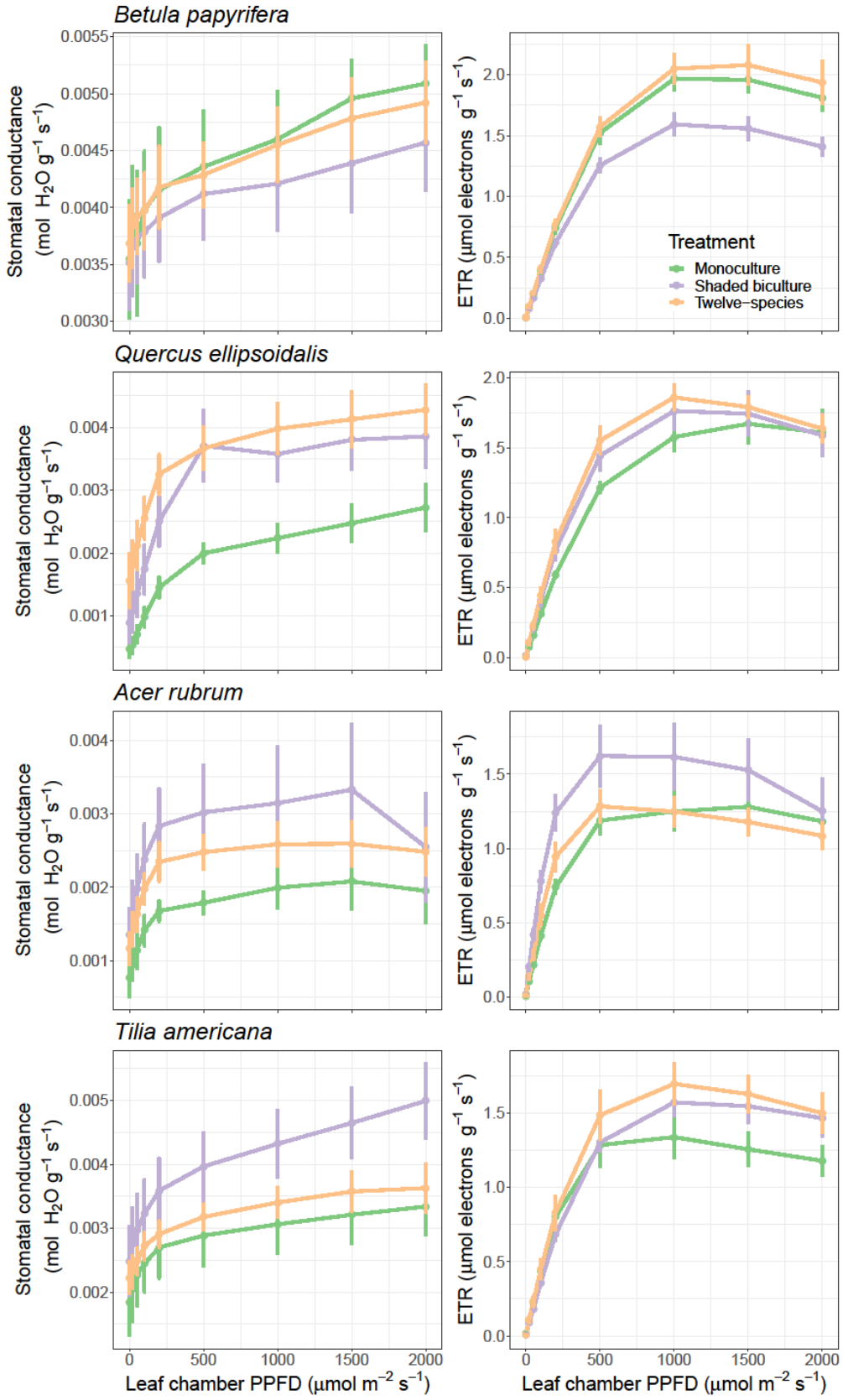
Betula papyrifera
Quercus ellipsoidalis
Acer rubrum
Tilia americana
Stomatal conductance (mol H2O g−1 s−1)
ETR (µmol electrons g−1 s−1)
Treatment
Monoculture
Shaded biculture
Twelve-species
Leaf chamber PPFD (µmol m−2 s−1)

Fig. S5

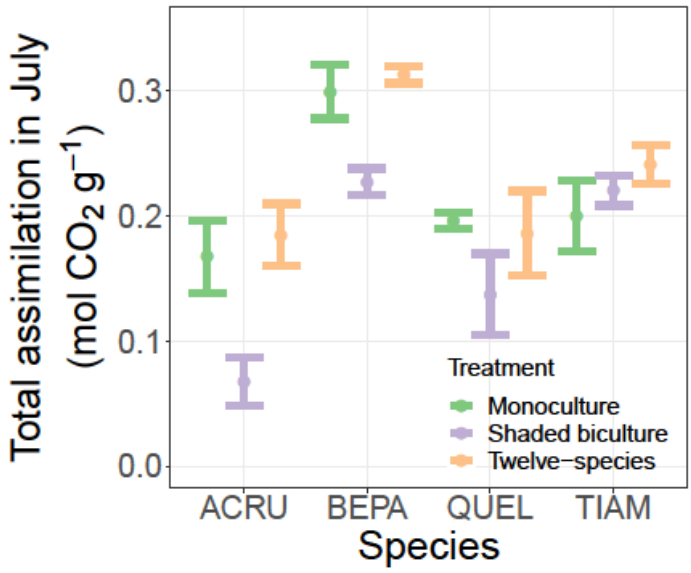
Total assimilation in July
(mol CO2 g−1)
0.0
0.1
0.2
0.3
ACRU
BEPA
QUEL
TIAM
Species
Treatment
Monoculture
Shaded biculture
Twelve−species

Fig. S6

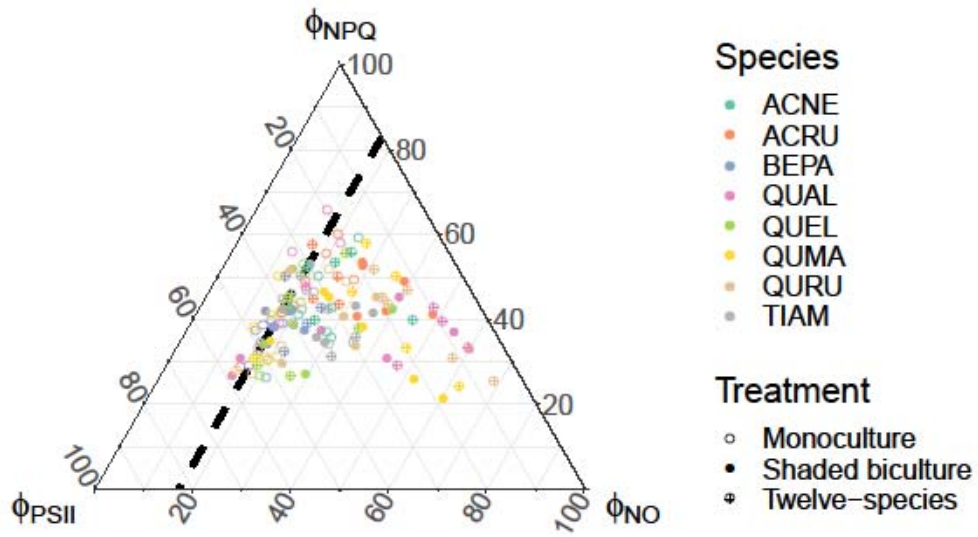
ϕNPQ
ϕPSII
ϕNO
20
40
60
80
100
Species
ACNE
ACRU
BEPA
QUAL
QUEL
QUMA
QURU
TIAM
Treatment
Monoculture
Shaded biculture
Twelve−species

Fig. S7

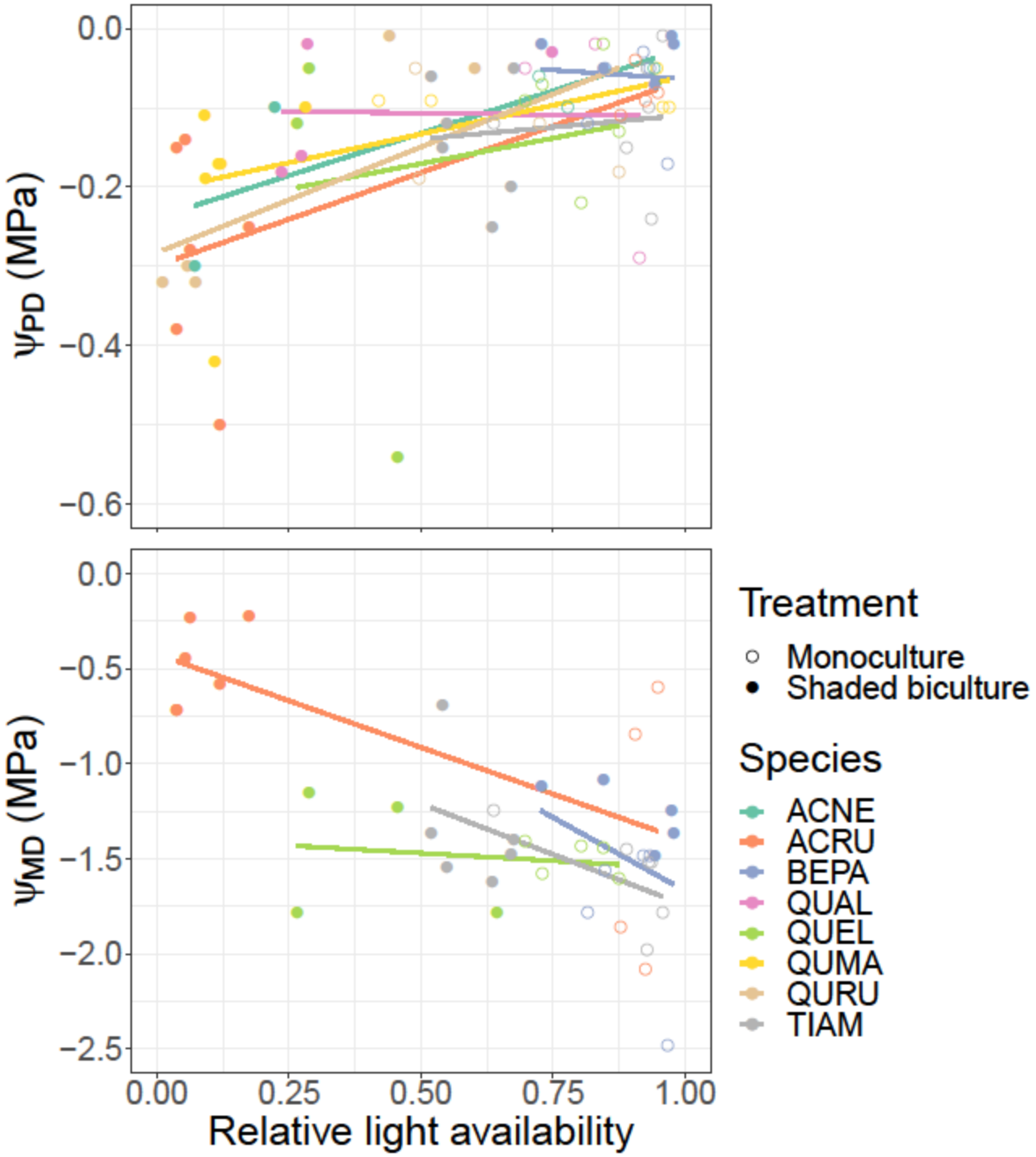
0.0
−0.2
−0.4
−0.6
ΨPD (MPa)
0.0
−0.5
−1.0
−1.5
−2.0
−2.5
ΨMD (MPa)
0.00
0.25
0.50
0.75
1.00
Relative light availability
Treatment
Monoculture
Shaded biculture
Species
ACNE
ACRU
BEPA
QUAL
QUEL
QUMA
QURU
TIAM